Quaternary Science Advances 14 (2024) 100190

Contents lists available at ScienceDirect

Quaternary Science Advances

journal homepage: www.sciencedirect.com/journal/quaternary-science-advances

Landscape evolution and hydrology at the Late Pleistocene archaeological site of Narabeb in the Namib Sand Sea, Namibia

Abi Stone [a,b], George Leader [c,d,b,*], Dominic Stratford [e,f], Theodore Marks [g,b], Kaarina Efraim [h,i], Rachel Bynoe [j], Rachel Smedley [k], Andrew Gunn [l], Eugene Marais [b]

[a] Department of Geography, School of Environment, Education and Development, University of Manchester, UK
[b] Gobabeb Namib Research Institute, Gobabeb, Namibia
[c] Department of Sociology and Anthropology, The College of New Jersey, Ewing, USA
[d] Department of Anthropology, University of Pennsylvania, Philadelphia, USA
[e] Department of Anthropology, Stony Brook University, Stony Brook, NY, USA
[f] School of Geography Archaeology and Environmental Studies, University of the Witwatersrand, Johannesburg, South Africa
[g] New Orleans Center for the Creative Arts, New Orleans, USA
[h] Department of Archaeology, University of Pretoria, Pretoria, South Africa
[i] National Museum of Namibia, Windhoek, Namibia
[j] Department of Archaeology, University of Southampton, UK
[k] Department of Geography and Planning, University of Liverpool, Liverpool, UK
[l] School of Earth Atmosphere and Environment, Monash University, Clayton, Australia

ARTICLE INFO

Keywords:
Namib Sand Sea
Middle stone age
Luminescence dating
Arid environment archaeology

ABSTRACT

The Namib Sand Sea (NSS) in Namibia is known to preserve a wide variety of Pleistocene-age archaeological sites. However, few Middle Stone Age (MSA) sites in this region have been systematically investigated and basic questions around chronology and technological organization remain open. Here we examine Narabeb, an open air MSA surface site exposed in an interdune pan, ~30 km into the northern NSS. Narabeb was first documented in the 1970s, and then re-examined in 2021 and 2022 by members of this team. Lithic technological analysis combined with a geomorphological description of the site, palaeoenvironmental interpretation of fine-grain water-lain sediments, and luminescence ages from northern and southern locations on the Narabeb pan provide some of the first understanding of human-environmental interactions and estimates of chronology from the later-Middle and Late Pleistocene in the NSS. In addition, we apply a quantitative approach to aeolian linear dune accumulation and extension to explore possible scenarios for landscape development at this site, in order to better understand the former water course(s) affecting the area. The new chronology suggests this site contained standing water at, or just after, the MIS 7/6 transition, and again at, or just after, the end of MIS 6 into early MIS 5. The timing of greater phases of water availability have some overlap with the speleothem growth record at Rössing Cave, situated ~90 km north of the NSS (and ~135 km north of Narabeb). Our results provide the foundation for larger, regional-scale analyses of early human adaptive strategies in this unique environment within Southern Africa.

1. Introduction

This paper presents the results of archaeological investigations at the site of Narabeb, a Middle Stone Age (MSA) surface site from the interior Namib Sand Sea (NSS) (Fig. 1). The NSS is the central sand-rich zone of the Namib Desert. The overall coastal Namib Desert extends from the Olifants River in South Africa to the Carunjamba River in Angola, and the NSS occupies ~34,000 km^2 between Lüderitz and Walvis Bay (Lancaster, 1989; Stone, 2013). While archaeological sites are known from the NSS, only a small number have been studied. The area is remote, overland travel presents an extreme challenge, and there are serious logistical barriers to access that have greatly hindered archaeological research in the area. Despite these obstacles, a number of surface-exposed sites have been identified that suggest hominins may

* Corresponding author. Department of Sociology and Anthropology, The College of New Jersey, Ewing, USA.
E-mail addresses: abi.stone@manchester.ac.uk (A. Stone), leaderg@tcnj.edu (G. Leader).

https://doi.org/10.1016/j.qsa.2024.100190
Received 25 January 2024; Received in revised form 7 April 2024; Accepted 17 April 2024
Available online 28 April 2024

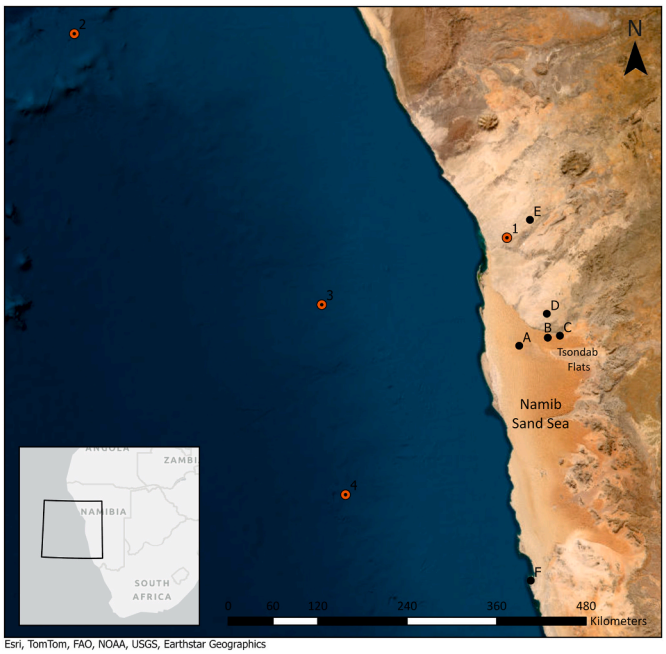

Fig. 1. Archaeological sites in the Namib Sand Sea and nearby, as discussed in the paper. A, Narabeb, B, Namib IV, C, Anibtanab (previously referred to as both Zebravlei and Mniszechi's Vlei), D, Mirabib, E, Erb Tanks, F, Tsau||Khaeb National Park (previously referred to as the Sperrgebiet). Also showing location of key palaeoenvironmental proxies for the region (used in Fig. 8), where: 1, Rössing Cave Speleothem (Geyh and Heine, 2014) and 2,3,4 are marine sedimentary cores containing proxies for terrestrial aridity: 2, MD98-2094 (Stuut et al., 2002), 3, MD08-3167 (Collins et al., 2014), 4, MD96-2098 (Daniau et al., 2023).

have occupied this region since at least the Middle Pleistocene (Shackley, 1980, 1982, 1985; Shackley et al., 1985; Leader et al., 2022, 2023). Surface sites such as these are challenging to date, which has hindered the ability to correlate occupations of the NSS into the broader framework of Southern African archaeology.

Surface sites make up the vast majority of all known archaeological sites in southern Africa (e.g. Hallinan, 2022; Coulson et al., 2022), the African continent and likely over the entire globe. By marginalising these types of site due to chronological ambiguity, tangible biases are introduced into the archaeological record that potentially result in unrepresentative interpretations of hominin behaviour and landscape use. Caves and rockshelters are valuable for establishing chronologies, but they represent only a small and geographically biased component of past hominin behaviour. Surface sites permit the investigation of human adaptive strategies on a much larger spatial scale than is available in rock shelter sites, and in this regard, we contend that they provide many opportunities that are complementary to traditional shelter-based records. Recent developments in chronometric methods and multidisciplinary investigations, such as those being conducted in the Middle Kalahari, and further south in the interior of southern Africa, alongside the one presented here, are beginning to explore these opportunities. Results include: MSA sites pre-dating and post-dating a ~72-57 ka palaeolake phase of Makgadikgadi in northern Botswana (Burrough et al., 2022; Coulson et al., 2022; Nash et al., 2022; Staurset et al., 2023a; b; Thomas et al., 2022; Thomas and Bynoe, 2023); MSA records of ~55 ka in the Karoo, northern Cape (Carr et al., 2023, 2024); MSA records ~77 ± 7-56 ± 6 ka in the Highveld of the Free State, South Africa (Wroth et al., 2022); and ESA and MSA archaeology in the Kgalagadi, southwest Botswana (Ecker et al., 2023).

At Narabeb there is a degree of chronological control for past environmental change based on existing quartz optically stimulated luminescence (OSL) ages obtained from paleohydrological research (Stone et al., 2010). In this study we target one sample from that same sedimentary sequence in (Stone et al., 2010), but measured using post-infrared infrared stimulated luminescence (pIR-IRSL) on K-feldspar, and also four new samples from a second location sampled in 2022. Our primary research aim is to clarify the chronological, palaeoenvironmental and behavioural context of human occupation in this region and we consider questions regarding how people may have adapted to the arid conditions through land use patterns, technological organization, and mobility strategies. In this investigation, we begin to address some of these questions and suggest directions for future research in the NSS.

2. Archaeological background of the Namib Desert/NSS

The Namib Desert is known to contain a wealth of Pleistocene archaeological material, but our understanding of Early Stone Age (ESA) and MSA occupations in the region derives from a handful of sites. The vast majority of known archaeological finds occur on the surface. Well-dated and deeply stratified sites are especially rare and therefore our understanding of regional chronologies is poorly developed (MacCalman and Viereck, 1967; Wendt, 1972, 1976; Corvinus, 1983, 1985 Shackley, 1980, 1982, 1985; Vogelsang, 1998; Dewar, 2008; Kinahan and Kinahan, 2010; Schmidt, 2011; Hardaker, 2011; McCall et al., 2011; Marks, 2015, 2018; Dewar and Stewart, 2016; Hardaker, 2020; Kinahan, 2022) (Fig. 1).

The best-studied stone-age site in the NSS is Namib IV, where, in the early 1980s, Myra Shackley reported the discovery of lithic artefacts and fossil faunal material on a lag surface of an interdune pan approximately 10 km south of the !Khuiseb River (Shackley, 1980, 1982, 1985). Lithics at the site were identified as typical of the Southern African ESA based on the presence of large cutting tools (LCTs) including handaxes, choppers, and associated flaking debris, knapped primarily on quartz and quartzite cobbles and pebbles. Her work also found mammal fossil bones embedded in a carbonate that she proposed to be contemporaneous to the ESA lithics. The fossils were assigned to *Elephas recki*. Based on these lithic and biochronological data as well as a single date on a mineralised fossil bone fragment from the site, Shackley et al. (1985) suggested a Middle Pleistocene age for the site, with >300 ka (a minimum age estimate, expressed as 347 +78, -48 ky BP for U-Th dating of a bone fragment, with some broadly supportive data from electron spin resonance (ESR) and racemization dating), whilst a biochronological interpretation of *E. recki* and other fossils suggested an age exceeding 500 ka (Klein, 1988; supported by Mesfin et al., 2021).

The identification of *E. Recki* at the site has now been questioned (Leader et al., 2023). More recent research suggests that *E. recki* may never have been present in this region of Africa (Todd, 2005). The purported *E. recki* fossils collected from Namib IV have since been lost, so it is not possible to re-examine this material to confirm or refute the identification or attempt new dating analyses. New research also suggests that Namib IV also contains a substantial previously unrecognized MSA component, including Levallois points and large blades, and typical MSA flake tools (Leader et al., 2023). The MSA-type material appears to be associated with distinct landforms compared with the ESA material at Namib IV, which suggests a complex depositional and erosional history and perhaps a later time frame of human use of the site (Leader et al., 2023). The stratigraphic and chronological association between the fossil beds and the stone tool-bearing areas is, as yet, unclear.

Shackley's research program identified MSA material in the NSS at the site of Anibtanab (previously referred to in the literature as both Zebravlei and Mniszechi's Vlei) (Fig. 1), located about 1.5 km south of the !Khuiseb River and about 40 km east of the Gobabeb research station (Shackley, 1985). Like Namib IV, Anibtanab is characterised as a lithic scatter exposed on an interdune pan surface. Shackley conducted a foot survey and observed a dense accumulation of lithic artefacts including points, blades, flake tools, large cores, and flaking debris knapped on quartzite and quartz cobbles. Anibtanab site was revisited in 2014 and

2021 and new lithic samples were described. These samples suggested that the site primarily consists of MSA-type material, with only a limited presence of diagnostic ESA-type material in the form of a single biface and several chopper cores (Leader et al., 2022). Portable X-Ray Fluorescence (XRF) data from quartzite artefacts at Anibtanab suggests that most of the lithics were knapped on raw material obtained from gravels within the !Khuiseb River valley itself and likely carried to the site (Marks et al., 2014).

Further to the south in the diamond-bearing region known as the Sperrgebiet or "forbidden zone" (now the Tsau||Khaeb National Park), in the late 1970s and early 1980s, G. Corvinus conducted an extensive archaeological survey as part of an environmental impact assessment for mining operations in the area (Corvinus, 1983). In her report, she described large volumes of handaxes, choppers and other ESA-type materials from former beaches raised by tectonic uplift. The assemblages were thought to be Early to Middle Pleistocene in age, but no radiometric dates were reported and no further investigations have since been conducted in the area. Furthermore, much of the material described exposures was later removed during diamond mining operations (Mesfin et al., 2022).

The MSA in the wider Namib region has been somewhat better studied. The best known site is the Apollo 11 cave in the Southern Namib, where, in the late 1960s and 1970s, E. Wendt, and later R. Vogelsang, documented a stratified cave sequence dating as far back as 63–70 ka using radioarbon and OSL techniques (Wendt, 1972; Vogelsang et al., 2010). The deposits at Apollo 11 contained evidence of Howieson's Poort and Still Bay-type lithic industries that suggested cultural connections with the wider Southern African subcontinent, where these industries are well known (Lombard et al., 2022). In the later occupations dated to c. 40-26 ka, Wendt also recovered a series of decorated stone plaques that are considered to be some of the earliest known representational art in Africa (Rifkin et al., 2016).

In the Central Namib gravel plains to the north of the NSS, Erb Tanks rockshelter yielded a stratified sequence of MSA materials dating to ~30-17 ka by OSL, with the lowest layers possibly dating as far back as 130 ka by Amino Acid Racemization (AAR) of ostrich eggshell fragments found in the lowest layers (McCall et al., 2011; Marks, 2018). Quartz OSL dates from the middle and upper MSA layers (Marks, 2018) suggest a rather late persistence of MSA technological modes in this part of the central Namib gravel plain compared to Southern Africa as a whole. The MSA layers at Erb Tanks yielded a MSA assemblage characterized by Levallois flakes and cores, as well as other typical MSA denticulates and other tools. No evidence of Howieson's Poort, Still Bay, or other chronologically diagnostic artefacts were found. However, a sourcing study enabled reconstruction of land use patterns and technological organization and highlighted how those patterns shifted at the end of the Pleistocene into the Holocene. Evidence from this study suggests the MSA occupations at Erb Tanks were characterized by a land use strategy focused largely on resources in and around the major river valleys and in the upland regions further to the east along the Great Escarpment. By the terminal Pleistocene and Early Holocene, this pattern appears to have shifted to a more dispersed land use strategy focused around semi-permanent water sources located farther afield from the ephemeral rivers (Marks, 2018).

3. Namib sand Sea: geological background

3.1. Geological history

The coastal Namib Desert belt is marked in the east by the Great Escarpment, which Brown et al. (1990) suggest started eroding as early as ~110 Ma (early Cretaceous). Burke (1996) argue for a later initiation of erosion, after ~30 Ma, following uplift of the mantle hotspot-driven Great Swell under southern Africa. An even later initiation (from ~23 Ma) is favoured by Picart et al. (2020), in their overview of planation surfaces on the Namibian west coast. It is worth highlighting three identified planation surfaces, Early-Miocene (~23 Ma), Mid-Miocene (~15 Ma) and Late-Miocene-Early-Pliocene (~5 Ma), because it is these events that will have transported large clasts east-west across the coastal plain, creating subaerially exposed cobble-rich surfaces north and south of our Narabeb study site. Underlying the unconsolidated NSS sands is the Tsondab Sandstone Formation (TSF) (Besler and Marker, 1979; Besler, 1996; Ward, 1988; Kocurek et al., 1999), which represents a consolidated-rock aeolian analogue of variable thickness (>200 m in the Dieprivier borehole and cliffs 40–200 m high) (Besler and Marker, 1979), stratigraphically assigned a Miocene age (Ward, 1984; Ward, 1987; Ward et al., 1983; Ward and Corbett, 1990), an age supported by large avian eggshell biostratigraphy (Senut and Pickford, 1995). There is evidence of fluvial incision of the TSF by the proto-!Khuiseb and proto-Tsondab Rivers (Marker, 1979; Ward, 1987; Eckardt et al., 2013a) associated with the formation of the ~15 Ma planation surface that is interpreted to have developed in a humid to very-humid, temperate climate (Picart et al., 2020). The calcified coarse-gravel conglomerate (Karpenkliff conglomerate) within the !Khuiseb River canyon, and observed in some interdunes south of Gobabeb, (Ward, 1987; Eckardt et al., 2013a) may be of this age.

3.2. Quaternary environmental history

The Quaternary climatic, environmental and landscape dynamics of the NSS are relatively poorly understood. Cosmogenic nuclide exposure suggests incision of the !Khuiseb River canyon starts ~2.8 ± 0.1 Ma, slowing down by ~0.44 ± 0.04 Ma (Van der Wateren and Dunai, 2001). The accumulation of unconsolidated NSS sands may have been occurring for 3-2 million years, based on estimates of modern-day sand input into the southwest of the NSS from the Tsau||Khaeb National Park/-Sperrgebiet, through to the Elizabeth Bay-Kolmanskop corridor of ~350,000 m^3/a (and total input of sand to the NSS of ~400,000 m^3/a) of Lancaster (1989). This is supported by cosmogenic-nuclide measurements of sands on a south-north transect suggesting a total residence time of sand along that transect in excess of 1 Ma (Vermeesch et al., 2010). The petrology, heavy mineral assemblages and zircon U–Pb spectra for the samples in the west, close to the coast, show a strong affinity with Orange River sands, whilst further east there is a strong fingerprint of sand deriving from rivers draining the Great Escarpment (Garzanti et al., 2012).

The NSS sands have been shaped into a wide range of dune morphological types (Livingstone et al., 2010). Our study region, and the focus of other sites previously targeted for dune dating, are dominated by complex linear dunes. There are ~60 luminescence ages from which to infer something about dune dynamics (Supp. Info. 1). Luminescence ages indicate the last exposure of sediment to light prior to burial, so we note that if the dune is migrating, or recycling sediment, the earlier phases of dune accumulation are not preserved. The oldest ages are in excess of 100 ka at both 0.5 and 6.5 m depths (Stone et al., 2010), noting quartz OSL is in saturation at this age (Supp. Info.1, column S, rows 30 to 42), and these are on western plinth of what is now a ~110 m tall complex linear dune on the east side of the Narabeb interdune (23°49′8.6″S, at our study site). Note that the dune plinth is the basal slope above the flatter interdune surface with a more consolidated texture than that found above, which has been termed the 'flank'. There is a later phase of aeolian accumulation recorded from 22.5 ± 1.4 ka to 15.6 ± 1.3 ka, also on a western dune plinth for sands 1–3 m deep further south in the NSS (~25°57′S) (Bubenzer et al., 2007). The eastern dune flank for the neighbouring complex linear dune to the west is 10.4 ± 0.7 to 9.0 ± 0.8 ka for comparable sediment depths, which led Bubenzer et al. (2007) to suggest a Holocene phase of activity reshaped the dunes, depositing sand on the eastern flanks of complex linear dunes.

Holocene dynamics are recorded as full-scale dune migration of complex linear dunes at the northernmost extent of the NSS. At "Visitor's", or "Warsaw Dune", 21 quartz OSL ages across nine boreholes, guided by a relative chronology from ground penetrating radar (GPR)

imagery indicates three phases of accumulation and migration from west to east (Bristow et al., 2007). The first is 5.73 ± 0.36 to 5.24 ± 0.27 ka, as a 'core', preserved on the west side of the dune and reaching ~20 m above the interdune surface, the second is 2.41 ± 0.10 to 0.14 ± 0.01 ka for the majority of the dune up to ~45 m elevation, and the third is very young (<52 years, expressed as ka before 2002 CE) for the uppermost ~5 m depth of sediment on the upper western flank and crest. The southeastern tip of the complex linear dune closest to the Gobabeb Namib Research Station ("Station Dune") (~2 km northwest) is also migrating over a Holocene timescale, but from east to west, with three quartz OSL ages for units guided by GPR of 1.57 ± 0.07, 0.99 ± 0.05 and 0.34 ± 0.02 ka, at 3.1, 4.8 and 3.3 m depths respectively (expressed as ka before 2002 CE) (Bristow et al., 2005). The two further ages from Chandler et al. (2022), ~10 km further south are: 0.11 ± 0.07 ka for western flank sands at 0.7 m depth, and 51.0 ± 7.8 ka at 0.61 m depth for an interdune sand unit. Further evidence for aeolian accumulation in the past few thousand years comes from quartz ages along a SSW-NNE transect of 12 sites across a complex linear dune (26°0′35.60″S to 26°0′29.77″S) (Stone et al., 2015). On the western flank ages range from 0.62 ± 0.03 to 1.39 ± 0.08 ka, across the crest, ages range from 0.08 ± 0.02 to 0.02 ± 0.02 ka, and on the eastern flank, ages range from 0.06 ± 0.04 to 1.85 ± 0.11 ka (expressed as years before 2013 CE) (Stone et al., 2015).

Insights into Late Quaternary dynamics of the !Khuiseb River come from the Homeb Silts and the Gobabeb Gravels, which have also been dated. The former have age estimates that range from 26 to 19 ka (Miyamoto, 2010) through to 9.8–9.3 ka (Bourke et al., 2003), whilst the latter have beds dated to 22 ka, 6.5 to 5.5 ka and as young as 600 to 300 years (Yamagata and Mizuno, 2005).

4. Study site and methods

4.1. Narabeb site

The Narabeb archaeological site occupies a long and narrow interdune pan approximately 30 km southwest of the Gobabeb Namib Research Station (Fig. 1). The near-flat interdune is ~500 m wide and is situated between large complex linear dunes, oriented approximately south-north. The climate today is hyper-arid (Eckardt et al., 2013b), with estimates of long-term mean precipitation of ~20 mm/a for the Narabeb weather station data from Lancaster et al. (1984). There is high interannual variability (Southgate et al., 1996; Eckardt et al., 2013b), and it is common for Narabeb to receive no annual rainfall. Estimated fog input is ~35 mm/a (Lancaster et al., 1984), which moves in from the

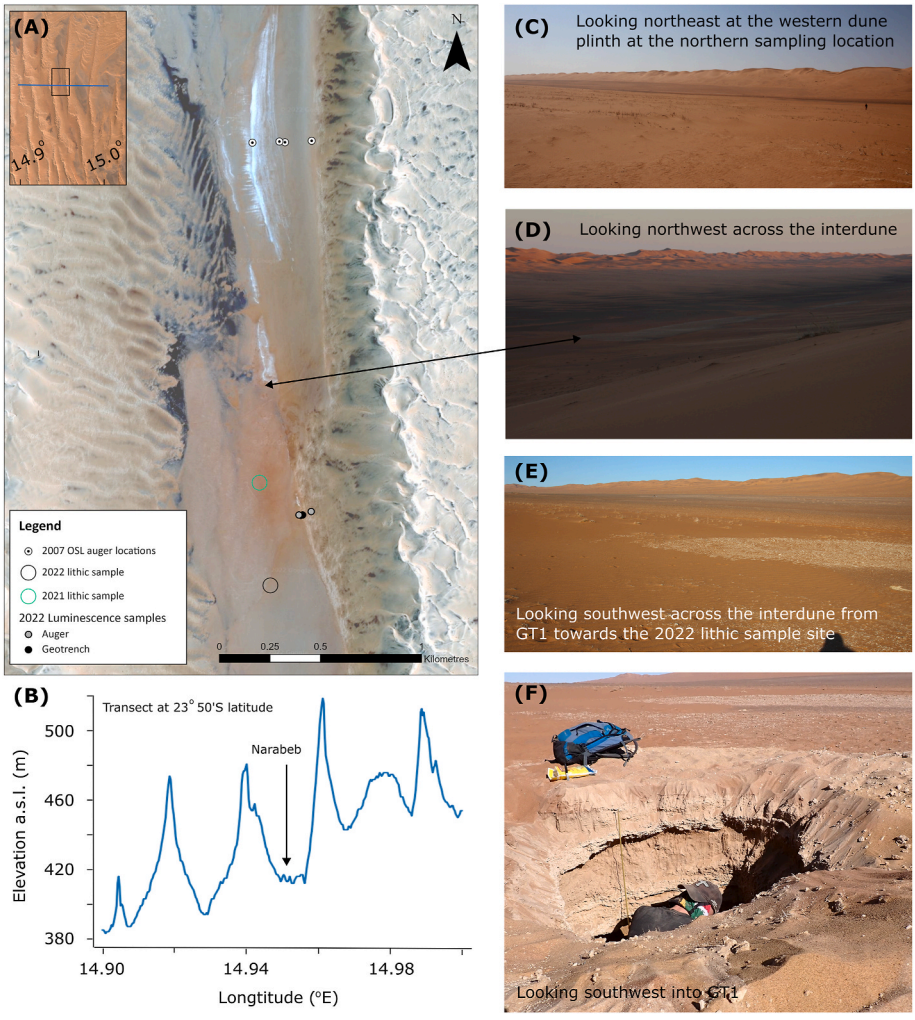

Fig. 2. (A) Narabeb sampling locations, northern location (2007 auger locations) and southern location (2022 luminescence samples), with (B) topographic transect at 23°50′S using AW3D30 (ALOS Global Digital Surface Model ALOS World 3D - 30m: Credit: AW3D, JAXA). Photos: (C) looking northeast at the 'shoulder' of sediment at the plinth location on the western dune flank, which is the northern sampling location (person for scale on RH side), (D) looking northwest across the interdune from the flank of the dune to the east of Narabeb (arrow indicates a point of reference with the satellite image), (E), looking southwest towards the 2022 lithic survey sample (people in distance for scale) from next to geotrench 1 (GT1) at the southern sampling location, (F) a view southwest into GT1 showing the carbonate-rich layers interbedded with sands.

coast (Eckardt et al., 2013b; Mitchell et al., 2020). Measured monthly evaporation rates at Gobabeb sum to >4600 mm/a (Lancaster et al., 1984), and PET (potential evapotranspiration) rates will be higher still.

Narabeb is west of the Tsondab Flats, a dune-free region where the TSF is exposed at the surface. The TSF has observable terrace topography, considered to be fluvial in origin and documenting the flow of the Miocene proto-Tsondab River westwards, towards the coast (Marker, 1979). The complex linear dunes in this region reach heights of 100–150 m with a wavelength (spacing) of between 1.5 and 2.5 km (Lancaster, 1989; Bullard et al., 2011; Livingstone, 2013). Secondary dunes consist of transverse-shapes (with a wavelength of ~100–200 m), oriented broadly west-east, on the lower slopes of the larger linear features, whilst the crests of the larger features contain curved shapes with a variety of orientations that often meet in star shapes (Fig. 2A). These secondary features are not identified well on a west-east elevation transect (Fig. 2B), partly owing to uncertainty in vertical resolution, and partly owing to the orientation of the secondary dune features in relation to the west-east transect.

The interdune surface at Narabeb has a thin veneer of fine to coarse pebble-dominated gravels locally overlying finer-grained, sandy sediments in linear wash zones. Five kilometers north and 10 km south of the Narabeb pan, and at higher elevations, abundant rounded and sub-angular cobble-sized silicate ('chert') clasts, with heavy upper surface desert varnish development, cover the surface. In the south, these cobbles create a significant pavement, likely representing deflation on a former terrace. The cobble-rich units are associated with alluvial fans or fluvial systems from the ancient Tsondab River course (e.g. Besler, 1996). Referring to Picart et al.'s (2020) model for planation surfaces, these are likely to be associated with either S7 (mid-Miocene, ~15 Ma, which is post-TSF accumulation) or S8 (late Miocene-early Pliocene, ~5 Ma). However, unlike the conglomerates located near the !Khuiseb River, there is no chronological control for the cobble units present in the Narabeb pan.

The curved white-surface feature seen in satellite imagery (23°49′29.18″S to 23°48′43.26″S) extends for ~1.4 km (Fig. 2A) and marks a slightly convex form in the landscape, with a flatter-top, described by Teller and Lancaster (1986) and Teller et al. (1990) as a 'bench' below the lower flank of the complex linear dune (Fig. 2C). This is found on the western plinth of the dune on the eastern side at this location. It is the same ~36 m thick 'section' reported by Seely and Sandelowsky (1974) that contains calcareous mudstone units, interstratified with sand units, where three (assumed basal) lacustrine carbonate samples were taken for U–Th dating by Selby et al. (1979). The section was studied later by Teller and Lancaster (1986, 1987) with the calcareous mudstones radiocarbon dated, and by Stone et al. (2010), who sampled and dated the sand-rich units that interstratify the water-lain mudstones. To the south, and at slightly lower elevation at the eastern edge of the interdune, there are further surface exposures of calcareous-rich sediment seen in the satellite imagery, which are ~200 m long, ~320 m long and ~50 m long (see Fig. 2D). The last of these is located between the our two archaeological sampling locations. The sediment exposures may correspond to some part of the thicker sequence to the north. It is not clear (or easy to reconstruct) the extent to which the interdune surface has been deepened by deflation following the deposition of this sequence.

Narabeb was initially visited for archaeological observations briefly by members of our team in 2013 during a reconnaissance survey and a high abundance of MSA artefacts was documented among the surface gravels across the surveyed interdune area. At the time, it was unknown whether the area contained any stratified deposits, but the absence of any ESA or Later Stone Age (LSA) artefacts was notable. Teller and Lancaster (1986) and Seely and Sandelowsky (1974) reported ESA material in the Narabeb area, with a highest concentration within ~2 km of the preserved water-lain sediments, but no ESA artefacts have been found in the area during this research. Some reported locations are challenging to identify, having been recorded in a pre-GPS period. No further archaeological research was undertaken until 2021 and 2022 when our team returned to conduct the investigations detailed in this paper.

4.2. Archaeological survey

Investigations began at Narabeb in 2021 with a preliminary survey driving north to south alongside the interdune plain to determine where major concentrations of artefacts lay on the surface. At three locations in the northern, central, and southern portions of the plain, we conducted simple foot surveys and observed artefacts appearing to be generally uniformly distributed across the entire area. To minimize selection bias, we divided an approximately 200 m long section of the interdune plain approximately halfway between the northern and southern ends of the pan into numbered 15 by 15 m grid squares and selected one of the squares using a random number generator (Sample 1, S23° 50.054′, E14°57.270′) (Fig. 2). Based on our initial observations, the density of artefacts in our sampling area appears to be representative of the average density across the entire site, though this needs to be confirmed with more extensive studies. Returning in 2022, we repeated the same sampling procedure at another location in the interdune plain (Sample 2, S23° 50.328′, E14°57.299') (Fig. 2).

In the selected grid squares, all artefacts on the surface were first visually identified and flagged, and then handled during in-field measurements and photographed before being placed back in the original location to the best of our ability. We classified each artefact according to a simple typology and collected standard measurements for length, width, thickness and mass based on widely utilized practices (e.g. Odell, 2004; Andrefsky, 2009). We also recorded the raw material type, number of flake scars and platform facets, and we visually estimated the cortical coverage for complete flakes and cores (Marks, 2018; Leader et al., 2023).

In addition to the intensive investigation of the sample survey squares, we conducted informal foot surveys of the surrounding interdune plain. In the course of these surveys, we identified a large number of tools, including most of the diagnostic artefacts (Fig. 3), but we did not include these in our measurements in order to preserve the random nature of the quantitative sample and minimize selection bias.

4.3. Luminescence dating

Stone et al. (2010) hand-augured profiles at four locations along a transect on the western plinth of sediments below the 'bench/shoulder' identified by Teller and Lancaster (1986) (from west to east these are NAM07/2, NAM07/1, NAM07/2 and NAM07/4) (Fig. 2, white circles for 2007 sampling locations in the northern sampling location). Sediment samples were prepared and analysed for quartz OSL dating at the Oxford Luminescence Dating Laboratory, using modal grain sizes for each sample, where the sand units in NAM07/1 were finer sand (90–150 μm) than the other profiles (210–250 μm) (see Stone et al. (2010) for full details). In 2022, we targeted a southern location between (laterally) the two archaeological survey samples, digging two pits (GT1 and GT2) in between surface exposures of calcareous-rich material and auguring the dune sand of this lowermost western plinth of the dune near the contact with the interdune and ~60 m east further up the plinth. In the field, the line of lighter imagery expressed at the surface contains fragmented, platy clasts, formed as the calcareous-rich unit weathers at the surface. Samples were collected using opaque tubes inserted into cleaned sedimentary profiles in GT1 and GT2 and using opaque tubes inserted into an opaque metal sampling head in the hand-auger for the two other locations on the dune plinth (D1 and D2).

The four 2022 samples and a fifth sample, NAM07/2/13, (a sample from 6 m depth in profile 07/2, un-dated in the study by Stone et al. (2010)) were prepared under subdued red lighting conditions at the University of Liverpool Luminescence Laboratory for D_e analysis using coarse-grain (212–250 μm) K-feldspar, given quartz luminescence

Fig. 3. Upper Left; MSA point from the pan surface outside the sample areas, Upper Right; flakes from Sample 1 location; Bottom; Centripital core from Sample 1 location.

signals were in saturation at the NAM07 (2007) sampling location. Samples were treated with a 10% v/v dilution of 37% HCl and with 20 % v/v of H_2O_2 to remove carbonates and organics, respectively, before dry sieving and isolation of K-feldspar using density separation. 2 mm diameter aliquots were measured using a Risø TL/OSL DA-15 automated system equipped with a $^{90}Sr/^{90}Y$ beta source (Bøtter-Jensen et al., 2003) fitted with a blue filter pack (BG39, BG3) in front of the photomultiplier tube. A single aliquot regenerative dose (SAR) protocol (Murray and Wintle, 2000) was used for the post-IR-IRSL analyses performed at 225 °C (Thomsen et al., 2008) (the $pIRIR_{225}$ signal). A preheat temperature of 250 °C for 60 s was used prior to stimulations of 100 s using the infra-red LEDs at 225 °C. An elevated temperature IR bleach of 290 °C for 200 s was performed at the end of each L_x/T_x cycle. The first 2 s and final 24 s of stimulation were summed to calculate the initial and background IRSL signals, respectively. Aliquots were accepted after applying the following screening criteria and accounting for the associated uncertainties: (1) whether the test dose response was greater than 3 above the background, (2) whether the test dose uncertainty was less than 20%, (3) whether the recycling ratios were within the range of ratios 0.8 to 1.2, and (4) whether recuperation was less than 5% of the response from the largest regenerative dose. Dose recovery tests were undertaken from three other NSS samples in this batch (1.00 ± 0.01, 1.02 ± 0.01 and 0.97 ± 0.01). Fading rates (g-values, Aitken, 1985) were determined for three aliquots of each sample and normalised to a t_c of two days (Huntley and Lamothe, 2001). The weighted mean and standard error for $pIRIR_{225}$ signals was −0.2 ± 0.7%/decade and given that the fading rates were negative with large uncertainties, and in line with previous studies using the $pIRIR_{225}$ signal (e.g. Roberts, 2012; Trauerstein et al., 2012; Kolb and Fuchs, 2018), we did not correct the ages for fading.

Calculations of environmental dose rates throughout burial for each sample used measurements of U, Th, K and Rb concentrations via inductively-coupled plasma mass spectrometry. Water contents were estimated considering the environmental history for each sample. An internal K-content of 10 ± 2% (Smedley et al., 2012) were used to determine the internal dose-rates (0.77 ± 0.15 Gy/ka). An a-value of 0.10 ± 0.02 (Balescu and Lamothe, 1994) was used to calculate the alpha dose-rates. Cosmic dose-rates were determined after Prescott and Hutton (1994). Dose-rates and burial ages were calculated using the Dose Rate and Age Calculator (DRAC) (Durcan et al., 2015).

4.4. Portable luminescence reader measurements

We use a Scottish Universities Research Centre portable luminescence reader (POSL or port-OSL) to measure the IR-stimulated and blue-stimulated luminescence signals from bulk sediment for all southern site samples, and the available remaining bulk sediments from the northern sampling location of Stone et al. (2010). The POSL signal size can give an insight into relative sample age, noting that the signals are mediated by a range of factors, including sediment texture (mean particle size and particle size distribution) and petrological variations between samples (Sanderson and Murphy, 2010; Stone et al., 2015, 2019; Stone et al., 2019; Munyikwa et al., 2021). We placed a mono-layer of bulk sediment into 5 cm petri-dishes, and used a POSL sequence of 15 s dark count, 60 s IRSL estimation (LEDs passed through an RG780 long pass filter), 15 s dark count (includes phosphorescence), 60 s post-IR blue-stimulated

luminescence (BSL) (LEDS passed through a CG420 long pass filter, and 15 s dark count (includes phosphorescence), where all emitted signals are filtered through UG11 filters. For data analysis we used the total signals over 60 s (minus the dark counts, inclusive of phosphorescence) for IRSL and BSL, and calculated the signal depletion index and the ratio of the IRSL:BSL signals.

5. Results

5.1. Archaeological survey

In total, we collected measurements on 302 lithic artefacts recovered from the two 15 × 15 m survey sample squares. Summary metric data for the assemblage is reported in Table 1. The assemblage was heavily dominated by flaking debris, making up more than 93% of the total collection. This includes unretouched complete flakes (40.3% of total, n = 122; Fig. 4), shatter (32.5% of total, n = 98), medial and distal flake fragments without platforms (12.9% of total, n = 39), and incomplete proximal flakes that preserve complete or partial platforms (7.3% of total, n = 22). Where it was possible to be determined, 78% of complete flakes preserved some cortex on their dorsal surfaces and averaged 2.1 removal scars per flake (1.8–2.4 95% CI). A histogram of cortical percentages for complete flakes is shown in Fig. 5. No refitting attempts were made in the field and artefacts were not removed from the site for study under laboratory conditions, as per the conditions of the research permit.

Core reduction strategies are dominated by centripetal and multidirectional techniques, with a small number showing unidirectional reduction. Centripetal cores (29.4% of cores, n = 6) are characterized by flake removals extending from the edge of the core inward toward the centre on one or both faces. Though we did not collect any "classic" struck Levallois cores in our grid sample, the large number of Levallois points observed elsewhere on the Narabeb pan surface gives us confidence that the cores in our sample likely represent Levallois-type reduction. Multidirectional cores (52.9% of cores, n = 9) show scars running in multiple directions across several faces and rotation of the cores in an irregular fashion. The small number of unidirectional cores (11.8% of cores, n = 2) are characterized by limited numbers of strikes from a single platform face and are probably best characterized as tested pebbles. Cortex was present on 92.8% of the cores where it was possible to determine. Cores also averaged 5.8 flake removals per core (5.0–6.6 95% CI).

Formal flake tools are typical of Southern African MSA assemblages (see Fig. 3). Tools were overall uncommon in the surface collected sample that was subjected to detailed study, with the total assemblage of tools consisting of a single denticulate, one notched tool, one bilaterally retouched Levallois point, and one unretouched Levallois point, together making up 1.3% of the total analysed assemblage. It is important to note that during an informal survey of the rest of the Narabeb site, we observed dozens of Levallois points and other typical MSA tools lying on the surface but these were not subjected to metric analysis to ensure the integrity of the randomized surface sample.

The sample of cores is quite small, so drawing larger conclusions about the *chaine operatoire* at Narabeb is challenging. The sample of unidirectional cores was too small to be subject to statistical testing and so here we compare only centripetal versus multidirectional cores. The centripetal cores were heavier than the multidirectional cores on average, though the difference was not statistically significant (two-sample difference of means test; $t = 1.4521$, $p = 0.1771$). The average number of scars per core also did not show significant differences between the centripetal and multidirectional cores ($t = 0.3737$, $p = 0.7164$). The difference in percentage of cortical coverage was *almost* significant at a 95% CI ($t = -1.5550$, $p = 0.0793$), with centripetal cores showing an average of 43% cortex coverage compared to 25% coverage on multidirectional cores. Centripetal cores averaged 137.9 cc in a simple 3-dimensional volume estimation compared to 46.6 cc for multidirectional cores. Again, however, this difference was almost -but not quite-significant at a 95% CI ($t = 1.7966$, $p = 0.1026$).

On the Narabeb interdune surface, subangular chert nodules between roughly 100g to 2 kg in mass are abundant, with the largest cobble-size clasts represented at the northern and southern extremities of the pan. The chert at Narabeb is most likely derived from fluvially reworked siliceous nodules that formed within the limestones of the Naukluft Mountains (Korn and Martin, 1959; Hartnady, 1978; Viola et al., 2006; Miller, 2008) ~50 km east of Narabeb in the Great Escarpment and transported to the area by the Tsondab River system during the Miocene. Based on our survey data, knappable chert clasts are not distributed across all interdune pans of the northern NSS, and are likely associated with the formation and exposure of Miocene fluvial gravel deposits. It is notable that more than 96% of the flakes, cores, tools, and debitage in the analysed sample were knapped on the chert that is locally available in the area. Two colour varieties of the local raw material were noted in the assemblage, brown and gray (Table 2), but these colour differences are almost certainly a consequence of surface weathering processes and for all practical purposes they are identical materials. No significant differences in morphology or mass were found across flakes, cores, and tools on the different brown and gray cherts.

Other raw materials were present but uncommon in the samples (Table 2). Four unretouched complete and incomplete flakes were found knapped on a black siliceous material that appears to be a fine grade of dolerite or hornfels. As with the chert, these lithologies are also found within the Naukluft Mountains basement rocks (granites and gneisses) of the Marienhof Series (Miller, 2008).

Quartz and quartzite are rare and absent, respectively, from the Narabeb sample, a pattern highly uncharacteristic of other known sites in the northern NSS region. At Namib IV and Anibtanab, quartzite and quartz are the most common materials in the surface assemblages (Leader et al., 2022, 2023), whilst they are conspicuously absent in the sample from Narabeb. Further to the north, large (~500 g–10 kg) subrounded to rounded nodules of quartzite and quartz are widely available in the !Khuiseb River valley, derived from the Oswater and Karpfenkliff formations exposed on terraces along the lower reaches of the river valley.

Table 1
Lithic types and sizes.

Type	n	Avg. Length (cm)	Avg. Width (cm)	Avg. Thickness (cm)	Avg. Mass (g)
Flakes and Debitage					
Flake	122	4.1	3.1	1.1	20.7
Flake Fragment	39	3.2	2.8	1.0	13.9
Incomplete Flake	22	3.1	3.4	1.2	21.0
Shatter	98	3.0	0.9	0.7	7.9
Cores					
Centripetal Core	6	6.0	5.5	2.9	128.5
Multidirectional Core	9	5.1	3.9	2.8	75.8
Unidirectional Core	2	4.4	3.9	2.7	62.0
Tools					
Denticulate	1	5.3	4.2	2.6	57.0
Levallois Point	2	8.1	3.6	1.3	47.0
Notch	1	5.1	3.0	1.1	27.0

5.2. Luminescence dating

The luminescence ages are shown in Table 3 with ± 1σ uncertainties, using the central age model (CAM) (the minimum age model (MAM) is also displayed for sample 07/2/13). The use of $pIRIR_{225}$ both changes previous chronometric interpretations at the northern sampling location, and adds chronology for the open-air archaeological deposits close to the southern sampling location. The K-feldspar $pIRIR_{225}$ age for 07/2/

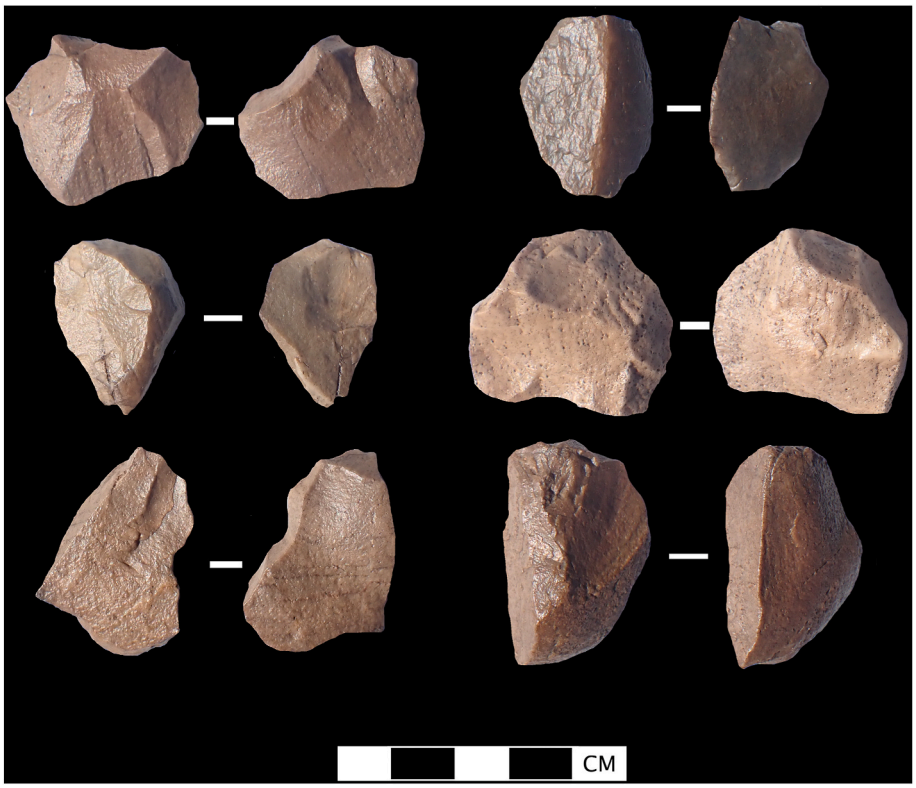

Fig. 4. A selection of flakes from Sample 2 at Narabeb.

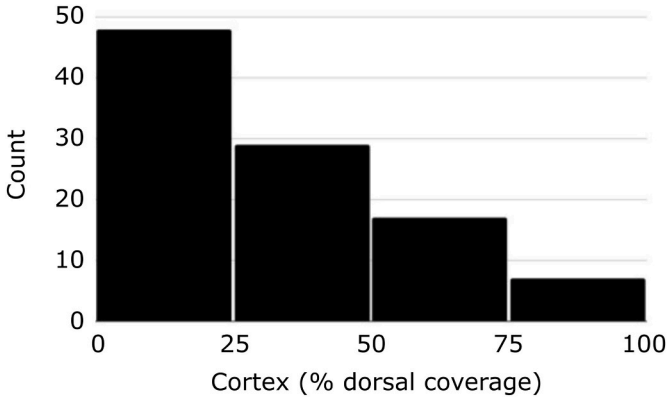

Fig. 5. Histogram of dorsal cortical coverage on complete flakes from Narabeb.

13 (CAM 223 ± 19 ka and MAM 206 ± 25 ka) confirms that the previous quartz OSL estimates for the majority of the northern sampling location (Stone et al., 2010) were minimum ages ($D_e > 2\bullet D_0$, where $2\bullet D_0$ is a seen as a prudent upper limit for quartz SAR dating (Wintle and Murray, 2006)) and represent a significant underestimation. For example, NAM07/2/14 at 6.5 m depth is > 115 ± 12 ka (quartz), compared to 07/2/13 (outlined above), which is 0.5 m above it.

The portable luminescence reader signals give some insight into the rest of the sequence at the northern sampling location (the ~36 m section of interbedded muds and sands) that has not been re-dated. The average total IRSL and BSL signals are lower for the sample in profiles 07/3 and 07/4 higher up the western dune plinth, which suggests they are younger than 07/2, within which the 07/2/13 sample has been dated in this study (Fig. 6A). It is also noteworthy, that the 07/3 samples in the middle of the profile, with the finer sedimentary texture have much lower total signals some with lower BSL depletion indices and one with a markedly lower IRSL:BSL ratio (Fig. 6A). This shows that where

Table 2
Raw materials of the lithics.

Type	Hornfels (n)	Gray/ Brown Chert (n)	Green Chert (n)	Quartz (n)	Grand Total (n)
Flakes and Debitage					
Flake	3	116	2	1	122
Flake Fragment		39			39
Incomplete Flake	1	21			22
Shatter		96	1	1	98
Cores					
Centripetal Core		6			6
Multidirectional Core		7	1	1	9
Unidirectional Core		2			2
Tools					
Denticulate		1			1
Levallois Point		1		1	2
Notch		1			1
Grand Total (n)	**4**	**290**	**4**	**4**	**302**

there is a marked sedimentary texture contrast the POSL signals are not a useful relative age tool (as also demonstrated for lake shoreline sediments by Stone et al. (2023) and Stone et al. (2024). For the southern sampling location the very young (0.9 ± 0.1 ka, expressed as ka before 2022) dune material has very low POSL signals, whilst the POSL signal size for the remaining three samples does not do a good job of distinguishing the K-feldspar $pIRIR_{225}$ ages (Fig. 6B). There is no obvious particle size driver of this pattern, or a driver from a shift in the IRSL: BSL, which might have indicated a petrological contrast (Stone et al., 2015, 2019; Stone et al., 2024).

Table 3
Luminescence dating results for the five samples dating using K-feldspar in this study, where four are from the southern sampling location from 2022 and one is from the northern sampling location, sampled in 2007 (Stone et al., 2010), alongside two existing saturated quartz age estimates from the northern location for context. For samples dated using K-feldspar (F), the internal K-content of 10 ± 2% (Smedley et al., 2012) yields an internal dose-rates 0.77 ± 0.15 Gy/ka. The latitude and longitudes for each sample is given in the Supp. Info. alongside abanico plots that show D_e distributions for each sample.

Sample code	Approx. elevation (m)	Depth from surface (m)	Q or (k)F	Grain size dated (μm)	U (ppm)	Th (ppm)	K (%)	External alpha dose rate	Ext beta dose rate	Ext gamma dose rate	Cosmic dose rate	Total dose rate (Gy/ka)	n	De (Gy)	OD	Ave 2 x D_0 (Gy)	Age (ka)
Northern sampling location																	
07/2/1	419.5	0.5	Q	180–210	0.98 ± 0.05	3.74 ± 0.34	1.59 ± 0.12	NA	1.17 ± 0.04	0.65 ± 0.01	0.18 ± 0.03	2.0 ± 0.1	18	>265.1 ± 28.2^{Q}	44	187	>132 ± 15
07/2/13	414.0	6.0	F	212–250	1.70 ± 0.5	9.20 ± 0.38	0.97 ± 0.10	0.11 ± 0.02	2.02 ± 0.11	0.79 ± 0.01	0.11 ± 0.03	2.8 ± 0.2	16	651.4 ± 34.6	22	1091	223 ± 19
														600.2 ± 62.9 ^{M}			206 ± 25 ^{MAM}
07/2/14	413.5	6.5	Q	210–250	1.69 ± 0.05	7.86 ± 0.38	1.35 ± 0.15	NA	1.18 ± 0.04	0.79 ± 0.01	0.11 ± 0.03	2.1 ± 0.1	16	>238.1 ± 23.3^{Q}	37	183	>115 ± 12
Southern sampling location																	
NA22/D2	417.5	0.50	F	212–250	0.09 ± 0.01	1.54 ± 0.15	1.75 ± 0.17	0.01 ± 0.00	1.30 ± 0.12	0.51 ± 0.04	0.28 ± 0.03	2.9 ± 0.2	17	2.6 ± 0.3	0	848	0.9 ± 0.1
NA22/G2	414.5	0.48	F	212–250	0.67 ± 0.07	3.75 ± 0.38	1.56 ± 0.16	0.06 ± 0.01	1.21 ± 0.13	0.60 ± 0.05	0.28 ± 0.03	2.9 ± 0.2	12	119.0 ± 2.9	8	841	41.2 ± 3.1
NA22/G1	414.0	1.10	F	212–250	0.36 ± 0.04	5.02 ± 0.38	1.49 ± 0.15	0.06 ± 0.01	1.20 ± 0.12	0.65 ± 0.05	0.26 ± 0.03	2.9 ± 0.2	12	395.3 ± 16.4	14	895	134.0 ± 10.8
NA22/D1	413.5	0.50	F	212–250	0.36 ± 0.04	3.76 ± 0.38	1.52 ± 0.15	0.04 ± 0.01	1.21 ± 0.11	0.59 ± 0.04	0.28 ± 0.03	2.9 ± 0.2	12	643.2 ± 31.7	16	862	231.0 ± 20.0

6. Discussion

6.1. Environmental context

6.1.1. Revised chronology for Narabeb

The paleoenvironmental interpretation of Teller and Lancaster (1986) for the thick sequence in the northern sampling location (where NAM07 samples were taken) remains unchanged. The seven calcareous-rich muds contain sedimentary features indicative of a low-energy lacustrine depositional environment (micaceous sediments, horizontally bedded and without features such as cross bedding and ripples indicative of flowing water). In addition, palaeoecological proxies are reported by Teller and Lancaster (1986), with diatoms only present in Unit IV, approximately Mud 3 of Stone et al. (2010) (Fig. 7). The eight species identified are indicative of a freshwater, high nutrient lacustrine environment. The seven sand units (above each mud) indicate a lowering of water depth (the water table may have dropped below the surface) during which aeolian sands accumulated. What does change significantly, using the K-feldspar $pIRIR_{225}$ age presented here for NAM07/2/13, is the estimate of the age of Sand 1, above the basal mud (Mud 1). This is 223 ± 19 ka (Table 3), which overlaps with the very end of the global MIS 7/MIS 6 transition, providing a minimum age for the basal mud (Mud 1) (Fig. 7). It is noteworthy that Selby et al.'s (1979) U–Th dates for Mud 1 are 210 ± 15 and 260 ± 25 ka (labelled in dark gray on Fig. 7). Of the radiocarbon dates provided in Teller and Lancaster (1986) (labelled red in Fig. 7) the ages 22,500 ± 2,800, 20,320 ± 300, 22,330 ± 600 and 26,400 ± 300 yr B.P. were proposed to represent the true depositional age for the sequence (whilst those in Mud 1 were thought to reflect an earlier wet phase and possible incorporation of older carbonate). Teller and Lancaster (1986) also argued that Selby et al.'s (1979) U–Th ratios from the calcareous mudstone reflected the age of bedrock from which the clays had been weathered. We suggest that the radiocarbon ages are too young, following Stone et al. (2010), because of a high likelihood of the incorporation of more-recent carbonate following the initial formation at this site, via recrystallization and post-depositional diagenesis.

At the southern sampling location, D1 is a sand-rich unit with only 2% silt (and a broad particle size distribution within the sand-sized fraction) (Supp. Info. 3), located on the dune plinth downslope of the surface calcareous-rich unit and close to the interdune. This is an aeolian unit, dominated by creep and saltation transport and deposition. Its platykurtic distribution is similar to particle size distributions for zibar and interdune samples reported by Lancaster (1981) and Lancaster and Ollier (1983), and much coarser than the finer (and more leptokurtic) particle size range for linear dune crests or slip faces (Supp. Info. 3). D1's age (231 ± 20 ka) overlaps within errors with the age for sand 1 at the northern sampling location, and D1 represents a maximum age for the water-lain unit upslope (and preserved in GT1 and GT2). This is further evidence for the presence of surface water at Narabeb at the MIS 7/MIS 6 transition. The Rössing Cave speleothem in the central Namib Desert (22°31′51″ S, 14°47′51″ E) contains a period of growth between 230 and 207 ka (U–Th dated), indicating a period of greater moisture availability in this record of intermittent speleothem and flowstone growth over the last 420 ka (Geyh and Heine, 2014) (Fig. 8). Stratigraphically higher in the western dune plinth sequence there is a sand-rich unit (with a very similar sediment texture to D1) (Supp. Info. 3) found at 1.1 m depth in GT1, which is beneath a calcareous-rich unit (Fig. 7). This sample, GT1, has an age of 134 ± 11 ka (Table 3, Fig. 7). This provides a minimum age for that water-lain unit, and this age overlaps with the global MIS 6/5 transition. There is a Rössing Cave speleothem growth period from 120 to 117 ka (Geyh and Heine, 2014), close to the timing of that water-lain unit (Fig. 8).

The sand-rich unit (with no silt) exposed in GT2 (Supp. Info. 3) is 0.68 m beneath a surface calcareous unit, and has an age of 41.2 ± 3.1 ka. Furthermore, it is only 1.4 m above the 135 ± 11 ka age in GT1, which indicates either that there was a very slow rate of (or episodic)

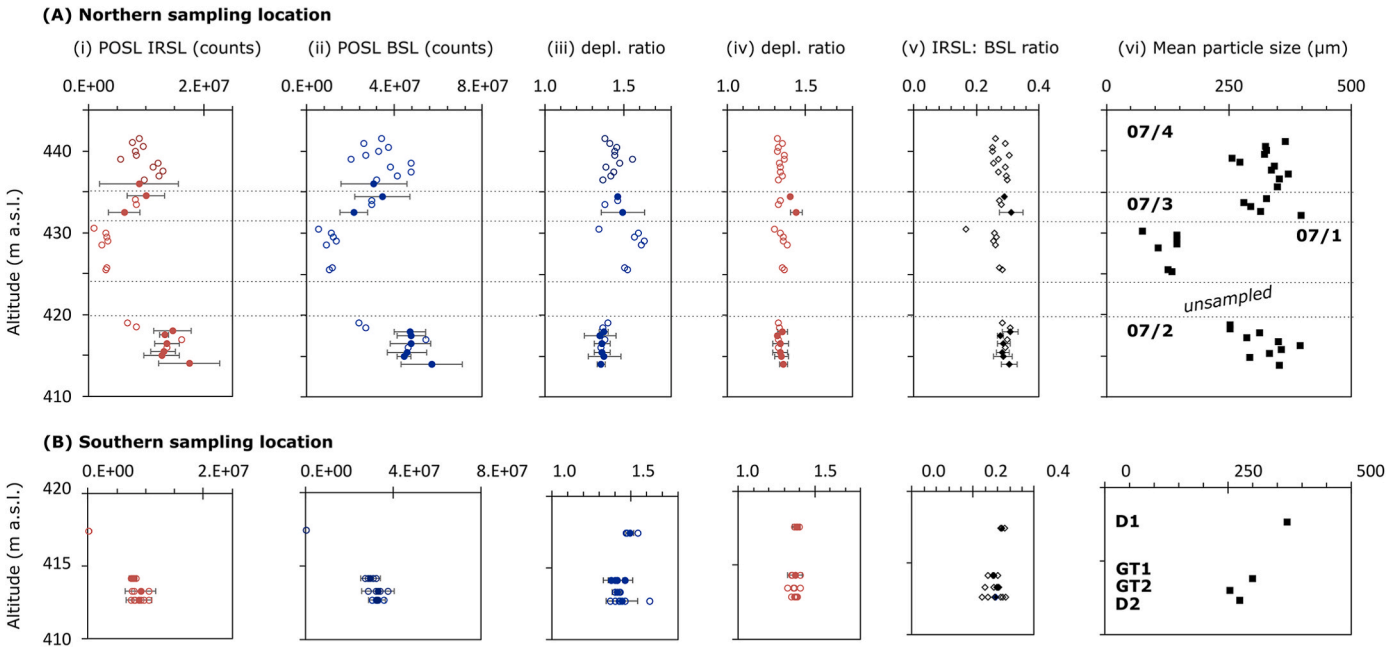

Fig. 6. Portable luminescence reader signal characteristics for the (A) northern sampling location and (B) southern sampling location, showing: (i) total IRSL signals, (ii) total BSL signals, (iii) depletion ratio of the IRSL signal, (iv) depletion ratio of the BSL signal, (v) the IRSL:BSL signal ratio. Mean particle size for the samples measured is shown in (vi). The y axis plots the data by altitude, rather than depth below the sloping surfaces from the multiple sampling locations, and in (A) the dashed horizontal lines indicate the four different augured profiles from Stone et al. (2010).

sediment accumulation at this site, and/or that there has been erosion of material in between the water-lain calcareous-rich units. The former is possible for a low dune plinth location with a limited sediment supply compared to sediment transport within the smaller secondary dune morphologies located along the crests of the complex linear dunes. However, it is also possible that sediment deflation and movement of sand along, or across, the interdune and lower dune plinth has occurred. The sand-rich unit at D2 (at 0.5 m depth and ~60 m east of the edge of the interdune surface) has an age of ~0.92 ± 0.13 ka (expressed as ka before 2022 CE). Thisrepresents a much younger phase of aeolian accumulation, and again indicates an overall low net accumulation rate of aeolian sand on the shallow plinth slopes of complex linear dunes in the NSS. The particle size distribution for this sample is platykurtic (20% coarse sand, 31% medium sand, 27% fine sand and 18% very fine sand, with ~2% coarse silt), and coarser in texture (Supp. Info. 3).

Our new chronology cannot resolve the age of the full accumulation history of the seven mud units in the ~36 m section in the northern sampling location (Fig. 7). However, the lower total POSL signals for samples in profiles 07/3 and 07/4 can be used to suggest that these sediments have a younger depositional ages than for 07/2/13 near the base (Fig. 6). This is supported by a non-saturated quartz OSL age of 68 ± 6 ka for the base of Sand 7 (NAM07/4/13) (Stone et al., 2010) (Supp. Info. 1), Nonetheless, further K-feldspar $pIRIR_{225}$ dating of the sand-rich sediments in that profile will be needed to better establish the timing of the middle portion of repeating muds and sands (Sand units 2 through to 7). For the Narabeb record as it now exists, the timing of the water-lain units correlated with the global MIS 7/MIS 6 transition and MIS 6/MIS 5 indicates substantially greater moisture availability in the NSS, and this is corroborated in the Rössing Cave speleothem growth record (Geyh and Heine, 2014) (Fig. 8).

The basal mud at the northern sampling location must exceed 223 ± 19 ka (07/2/13 in Sand 1), whilst the lowest water-lain unit at the southern sampling location must be younger 231 ± 20 ka (the lowermost dune plinth age D1). These timings coincide with a phase of inferred humidity for the terrestrial environment from aridity index of Stuut et al. (2002) for marine core MD98-2094 (Fig. 8), which is based on an interpretation of particle size of terrestrial-derived sediment flux. The water-lain carbonate-rich unit at GT1 is <134 ± 11 ka (based on the age of sand below), and three of the South Atlantic marine sediment core proxies relating to terrestrial aridity also indicate a wetter phase at this time (Fig. 8). These proxies are the aridity index from MD98-2094 (Stuut et al., 2002), the $\delta D_{n\text{-alkane}}$ leaf wax proxy in MD08-3167 (Collins et al., 2014) and the charcoal record of MD96-2098 (Daniau et al., 2023).

The hypotheses for the drivers of wetter phases on the western coast of Namibia include: (i) tropical African summer rain belt expansions during global interglacials, compared to glacials (Collins et al., 2011, 2013); (ii) expanded summer rainbelt with monsoonal precipitation originating from the Indian Ocean (Brook et al., 1997), with a precessional forcing; or (iii) a mechanism relating to conditions in the southern Atlantic connected (in-phase) to hydroclimatic conditions in the Northern Hemisphere, so that wetter conditions in the Namib Desert occurred at the same time as wetter conditions in the Northern Hemisphere tropics (Chase et al., 2019). Our Narabeb record is not continuous enough to assess conditions through full glacial-interglacial cycles, however, the ages at transitions suggest these were times with increased moisture availability (and possibly with fluctuations). The Narabeb ages could equally be interpreted as aligning with some of the precessional-paced peaks in austral summer (December) insolation (Fig. 8).

6.1.2. *Landscape evolution at Narabeb*

The process by which water reached and pooled at this site is also debated, involving either surface flow along a former Tsondab River course, or via groundwater seepage, or a combination of these hydrologically-related processes. The TSF acts as an aquifer (Christelis and Struckmeier, 2001), which further north in the !Khuiseb dune area (the area south of the !Khuiseb River towards the west coast) has a hydraulic conductivity of 4 m^2/day (BGR, 1998). The presence of freshwater springs at discrete locations close to the coast in the NSS, west of the Tsondab and Sossus Vleis suggests that there may be linear, alluvial aquifers, fed by 'up-stream' recharge through the former river valleys in the past and by modern-day recharge that enters the aquifer in the east, closer to the Great Escarpment, near the headwaters of the river systems.

Whilst Teller and Lancaster (1986) and Teller et al. (1990) concluded

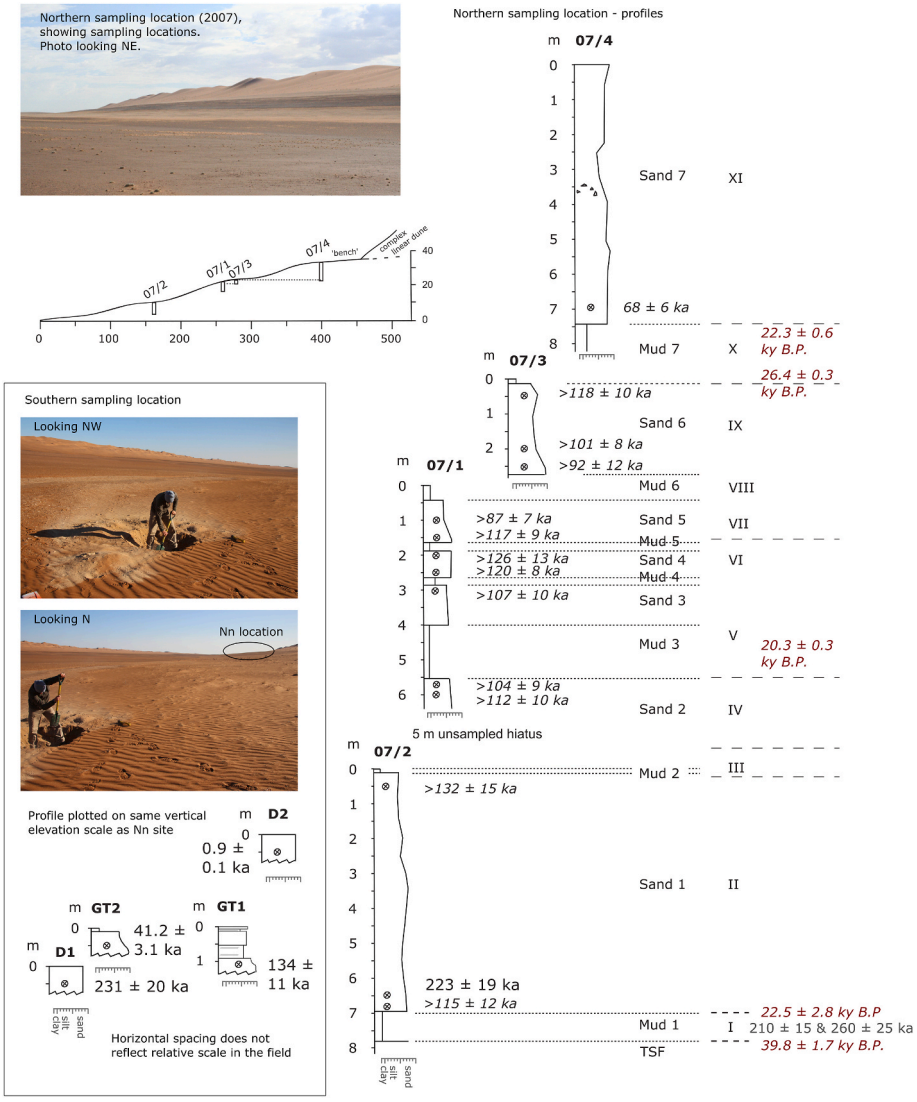

Fig. 7. Stratigraphy and age control for the northern (2007) and southern (2022) sampling locations at Narabeb, where dark gray label for Mud 1 is the U–Th dates on carbonate by Selby et al. (1979), the red labels are the un-calibrated radiocarbon dates on sedimentary carbonate in the muds provided by Teller and Lancaster (1986) provided by J. Vogel, the small italicized labels are the quartz OSL ages provided by Stone et al. (2010) that are in saturation, and the large black font are the K-feldspar pIRIR$_{225}$ ages provided in this study. The stratigraphic profiles for the northern and southern location are plotted on a common vertical axis (but there is no corresponding horizontal axis). Note the total of 14 units (7 sands and 7 muds) encountered by Stone et al. (2010) does not map one-to-one with the eleven (I to XI) units described by Teller and Lancaster (1986). (for interpretation of the references to colour in this figure legend, the reader is referred to the Web version of this article)

groundwater discharge from the TSF might have contributed some water to Narabeb, they proposed that the sedimentology and stratigraphy of Muds 1 to 7, along with the abundance of mica (which does not tend to survive in an aeolian environment), indicates that water flowed east-west across the surface of the Tsondab Flats. If there was flow along a former Tsondab River course ~230-210 ± 20 ka and ~134-125 ka there are a number of possible scenarios for landscape evolution. These are that: (i) the complex linear dunes were absent, at least to the east of Narabeb (as considered by Teller and Lancaster, 1986); (ii) the complex linear dune against which the sediments are found was present and the Tsondab River flowed in a course further north, periodically flooding from north to south down into the interdune; and (iii) the complex linear dune was present, but fragmented, for example at the break in the linear patterning seen at 23°51′51.98″S, implying a more southerly route and flooding the interdune from south to north.

It is possible to start to evaluate the different hypotheses using the quantitative approach of Gunn (2023) for aeolian landscape change through time. This uses: (i) the Advanced Land Observing Satellite (ALOS) Global Digital Surface Model (Tadono et al., 2014) (~30 m horizontal resolution and 1 ± 5 m vertical resolution) to estimate equivalent sand thickness (EST) for our linear dune geometry (Supp. Info. 4); and (ii) European Centre for Medium-Range Weather Forecasts Re-Analysis (ERA5)-Land climate data (which spans 1981 to 2020) (Muñoz Sabater, 2019) to estimate saturated sand flux (Qs) and its direction (Supp. Info. 4, Eq S4.1 to S4.6). Together, these allow us to estimate the rate that sand has accumulated in the region through time (Tη) (Eq. (1)):

$$T_\eta = EST \Big/ \left(\delta_\eta / \delta_t\right) \quad (1)$$

Within this, with find EST to be 11.26 m for the Narabeb region (north-south range 23.88°S to 23.78°S and east-west range 14.90°E to 15.00°E), which is calculated using the average dune relief in the area (dune and interdune) (Wasson and Hyde, 1983) and accounts for the local slope in the region (see Supp. Info. 4.1). The term ($\delta\eta/\delta t$) represents

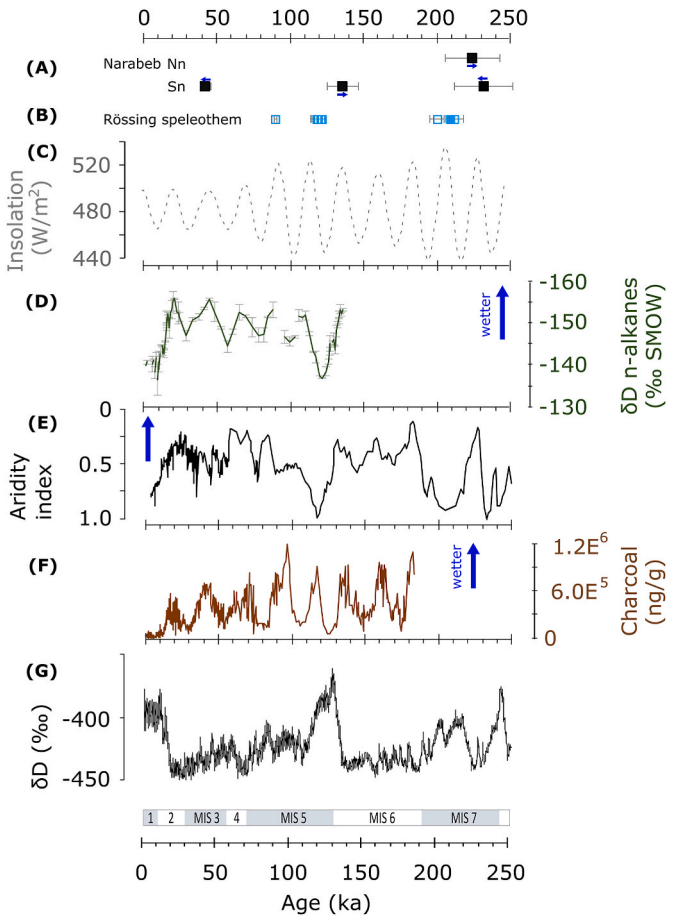

Fig. 8. (A) Narabeb K-feldspar pIRIR$_{225}$ ages plotted alongside (B) U–Th growth phases for the Rössing Cave Speleothem (Geyh and Heine, 2014) (C) insolation for December at 25°S (Laskar et al., 2004), alongside three marine sediment core proxies for humidity-aridity fluctuations from the South Atlantic, where: (D) is MD08-3167 $\delta D_{n\text{-alkane}}$ leaf wax proxy (Collins et al., 2014); (E) is MD98-2094 particle-size based terrestrial aridity index (Stuut et al., 2002) and (F) is MD96-2098 charcoal record (Daniau et al., 2023). (G) is δD from Epica Dome C in Antarctica (Jouzel et al., 2007).

the change in average elevation (η) per (unit) time (t), in which we are inferring the sediment accumulation and erosion rates due to spatial flux convergence and divergence at given locations (see Supp. Info. Eq. S4.5 (the Exner equation)), and we find this to be 54.08 mm/ka. This gives us 208 ka for T_η. This is the broad average rate it would have taken, under modern climatic conditions, to accumulate the amount of sand observed in the region for which we calculated EST, and this can be considered as an estimate for both dunes and interdune sand cover near to Narabeb.

It is also possible to estimate the elongation rate of linear dune (c) in m/a using Eq. (2) from Charnay et al. (2015):

$$c = \left|\overrightarrow{Q_{s,net}}\right| \Big/ \langle H \rangle \phi \tag{2}$$

where, $\left|\overrightarrow{Q_{s,net}}\right|$ is resultant drift potential (Eq. S4.6), $\langle H \rangle$ is the average dune height across the whole width of the dune and ϕ is the grain packing fraction (with (1-Φ) representing the air space/porosity of the sand dune). For the dune east of the Narabeb interdune site, $\langle H \rangle$ is 20.80 m (for the length between 23.84°S and 23.80°S). $\langle H \rangle$ is not to be confused with dune height at the crest, which is ~110 m high (Fig. 2B). Using the ERA5-Land climate data inputs we find $\left|\overrightarrow{Q_{s,net}}\right|$ to be 3.86 m^2/a (Supp. Info. 4, Eq. S4.6). This gives our linear dune elongation rate as 0.309 m/a. This would mean it took the eastern dune, of the dimensions we see today, ~26 ka to elongate from the 2022 luminescence sampling locations to the current end point of the dune, found ~8 km further north (Fig. 2A). Together, these estimates for the slow vertical accumulation of sand in the Narabeb region, and the rate of elongation of a complex linear dune such as that on the eastern edge of the interdune, could be used to support the idea that the landscape was either free of, or had much smaller dunes, around the times indicated for ponded water at the site from the new luminescence chronology. This lends support to scenario (i) of no dunes being present to the east of Narabeb.

However, the scenario of dunes in place (number iii), of some morphology and dimension, cannot necessarily be discarded. It is necessary to think critically about the assumptions used in this approach in order to model the accumulation of the complex linear dunes, not least assuming that the wind conditions and sediment availability of the last 40 years can be assumed to be representative of >200,000 years of the late Pleistocene. We must also recognize that these are complex linear dune features with superimposed secondary features, and that these wind data do not account for modifications to wind flow induced by flow-form interactions over these large dunes. These modifications to wind would change the nature of wind flow at the site in comparison to what is captured in the equations. Gunn et al. (2022, p2) highlight that when dunes reach sufficient dimensions to "perturb the [atmospheric] flow nonlinearly" the rules for what regulates the size, accumulation and migration of dunes, "becomes more complicated."

It is worth considering the ~60 m high Visitors Dune west-east lateral migration is reconstructed from luminescence-dated GPR-inferred stratigraphic units, and is an average of 0.13 m/a over the past 6 ka (Bristow et al., 2007). Visitors Dune is ~55% the height of those surrounding Narabeb, mathematically modelled here to have an extension rate of 0.309 m/a. These rates are in the same order of magnitude, albeit in the contrasting directions. Bristow et al. (2007) were not able to quantify a north-south elongation rate owing to the orientation of their GPR profile and sampling strategy.

Away from the chronology for these complex linear dunes closest to the !Khuiseb River, the only other insights we have about phases of linear dune accumulation within the current luminescence database for the NSS (Supp. Info. 1) derive from two locations in the south of the NSS. This reveals that there is complex linear dune sediment in excess of Holocene age, but only on a western facing dune plinth, where, at 3 m depth, the depositional age is 22.5 ± 1.4 ka (Bubenzer et al., 2007). In comparison, the eastern flank of the neighbouring dune is only 10.4 ± 0.7 ka (Early Holocene) at 4 m depth (Bubenzer et al., 2007). The second location provides further evidence for very late Holocene activity (maximum age 1.9 ± 0.1 ka, expressed as ka before 2013 CE) of shallow depths of sand (mostly 1 m depths, with two samples at 3 m depths) on a west-east profile across a complex linear dune (Stone et al., 2015). There is clearly a need for further luminescence dating of dune features in the NSS to gain a better understanding of past landscape dynamics.

6.2. *Archaeology*

Though the lithic sample size at Narabeb is small and our study should be considered as presenting preliminary data, there are interesting aspects that warrant consideration. At Narabeb, we see an MSA assemblage that is rather typical in the broad context of later Pleistocene Southern Africa. Based on the high proportion of cortical flakes and cores (Table 1) and the abundance of raw material in the immediate vicinity, it appears that tools were largely knapped on the site as opposed to being carried in from other locations.

It is difficult to formulate a scenario in which a human presence is possible at Narabeb without access to a nearby source of water. Therefore, we hypothesize that human occupations of the site may have coincided with periods of water ponding in the interdune area. Based on geomorphological analysis and luminescence dating, there are two main phases with wetter conditions, 230-220 ± 20 ka and after ~135 ± 10 ka, with some further, minor water-lain sediment at the southern

sampling location after ~41 ± 3 ka (GT2 southern sampling location). The two older ages are consistent with the typological characteristics seen in the artefacts at Narabeb, although we should be cautious in taking this line of reasoning too far, as the relationship between the lithics on the surface and sediments below the surface is still uncertain, except that the lithics must have been deposited after the sediments. Currently, we are not able to discern the degree of deflation of the interdune surface. This chronology (revised from Stone et al., 2010) represents the best estimates yet published for an MSA site in the NSS and can be considered a working hypothesis for developing chronologies through future research. Further $pIRIR_{225}$ ages for the entire ~36 m profile at the northern sampling location might reveal further details of the rate of accumulation of all seven muds and sands.

Considering the broader landscape scale, the spatial patterning of archaeological sites in the NSS suggests a complex history of occupation in the region. Notably, certain interdune zones and dry pans, like Narabeb and Namib IV contain abundant artefacts, while others in apparently identical environmental circumstances contain virtually none. For example, Hartmut's Pan, located only a few kilometers to the northeast of Narabeb is on an enormous open plain with similar evidence of periodic localized surface water flow and abundant lithic raw materials, yet we were able to observe only 3 or 4 possible lithic artefacts over an area of tens of square kilometers. No evidence of more modern erosion and removal of sediments and artefacts was noted, suggesting a similarly well-established interdune surface. This variation in site distribution suggests that there may have been a complex interplay between the availability of water resources (such as size, and duration of surface ponded water) and the spatial distribution of lithic raw material, which is controlled by the location of cobble-rich deposits moved in the Miocene phases of planation and fluvial deposition. These geomorphic and environmental factors structure the patterning of archaeological sites in the northern NSS.

It is notable that in both our systematic study and extensive informal survey at Narabeb, we did not encounter any evidence of ESA-type material at the site. This is in strong contrast to Namib IV (Leader et al., 2023) and to a lesser degree, Anibtanab (Leader et al., 2022). Though others (Teller and Lancaster, 1986) reported ESA in the Narabeb area, this may have been at a not-yet-rediscovered pan nearby. The absence of ESA may be due to the Narabeb's location deeper within the NSS. It is possible that, as it is today, the vicinity of the former Tsondab River valley may have been a less favourable habitat compared to the !Khuiseb River valley during earlier periods of the Pleistocene, becoming more habitable and attractive by the later Pleistocene.

Patterns of raw material use at Narabeb and comparison with other known sites in the northern NSS can give us some insights into land use patterns by later-Middle to Late Pleistocene MSA groups in the region. As discussed above, raw materials at Narabeb assoicated with the Tsondab River are heavily dominated by cherts (and hornblende) available in the immediate vicinity of the site, with only scant representation of other materials (Table 2). In contrast, quartzite and quartz dominate the MSA assemblages at sites such as Namib IV, Anibtanab, and Tsondab Route (Shackley, 1985), all located closer to the !Khuiseb River valley. This contrast in raw material usage, with strong distinctions between sites within different river catchments is suggestive of a land use pattern in which populations were moving largely east-west or west-east, possibly following rivers, or regions with potential ponding water (through flooding or ground-water seepage), through the desert, with relatively little movement north-south through the dunefields between these zones. East-west movement would have been much easier if dunes were not well developed during the MSA in the NSS, in contrast to modern conditions in which the tall, long, north-south complex linear dunes are harder to cross.

Keeping in mind the small sample size and the lack of statistical significance, we still believe it is reasonable to suggest that the centripetal cores represent an earlier stage of the sequence of reduction compared to the multidirectional cores. Core reduction at Narabeb proceeded on a trajectory where cores were initially shaped centripetally for the production of Levallois flakes and points with subsequent multidirectional reduction to produce expedient flakes from smaller cores before exhaustion.

7. Conclusion

Early human-environmental interactions are challenging to study and interpret even in well-stratified contexts. As a surface assemblage in the interior of the NSS, Narabeb presents further challenges associated with surface lithic assemblages in a landscape where deflation of former surfaces is possible. However, it is the current aridity in this landscape that makes the site important to understand because aridity acts as a natural deterrent for long-term occupation and a challenge for even short-term resource exploitation.

The samples of lithics represent MSA technology that likely spans several phases of use. We cautiously assume that the most likely time frame of occupation of the site is concurrent with the presence of ponded water in the Narabeb interdune – corresponding with the most likely wet phase(s) dated to 230-220 ± 20 ka and after ~135 ± 10 ka. This chronology for increased moisture availability has some overlap with dated growth phases in the Rössing speleothem. We therefore hypothesize that this locale was visited during these periods, at which time stone technology from locally sourced chert (and hornfels) cobbles were knapped. Under current conditions, the Tsondab ponds up ephemerally ~45 km SSE of Narabeb. It is possible to envisage a range of related scenarios where water from a former Tsondab River course reaches this site, whether directly from the east across a dune free surface, or involving some north-south (or south-north) flooding onto an already-existing interdune with a geomorphological association with Miocene fluvial planation and possible additional contributions of groundwater processes.

The occupation of the site appears to be largely confined to this range of time based on the technology present. While other interdune pans in the NSS have ESA technology, none has been found at the Narabeb pan. This further supports our hypothesis that this location, deeper in the interior of the NSS than other known sites, was only feasibly occupied during periods when water would reach this location. Narabeb demonstrates the potential for humans to enter and occupy an otherwise arid environment during windows of opportunity with greater moisture availability. The Tsondab River, or possibly other sources of water, may have been able to support minimal vegetation, though the extent is unknown. This, however, appears to have been enough for humans to move through this environment during the MSA. We aim to expand this research throughout the NSS and particularly along the Tsondab River. This will provide a clearer understanding of the movement of early humans - and hominins - into this now arid landscape, and of the environmental conditions that allowed them to do so.

CRediT authorship contribution statement

Abi Stone: Writing – review & editing, Writing – original draft, Formal analysis, Data curation, Investigation, Conceptualization. **George Leader:** Writing – review & editing, Writing – original draft, Methodology, Investigation, Conceptualization. **Dominic Stratford:** Writing – review & editing, Writing – original draft, Investigation, Formal analysis, Conceptualization. **Theodore Marks:** Writing – review & editing, Writing – original draft, Methodology, Investigation, Formal analysis, Data curation, Conceptualization. **Kaarina Efraim:** Investigation. **Rachel Bynoe:** Writing – review & editing, Methodology, Investigation. **Rachel Smedley:** Formal analysis. **Andrew Gunn:** Writing – review & editing, Formal analysis. **Eugene Marais:** Investigation.

Declaration of competing interest

The authors declare that they have no known competing financial

interests or personal relationships that could have appeared to influence the work reported in this paper.

Data availability

Data will be made available on request.

Acknowledgements

This research was funded by a Leakey Foundation Grant (GL). Funding towards travel for AS was obtained from a Quaternary Research Association small grant, and the University of Manchester SEED New Horizons Research Simulation Fund. The latter was also used for the costs of collaborative luminescence dating sample preparation and analysis with RS at the Liverpool Luminescene Laboratory, for which Dr Kaja Fenn and Luke Glascott are thanked for their help. Thanks to Dr Tom Bishop in the Geography Laboratories at the University of Manchester for guidance in analysis of laser granulometry raw datasets. This research was undertaken with the assistance of resources and services from the National Computing Infrastructure (NCI), which is supported by the Australian Government, through grant NCMAS-2024-105 to AG. Thanks to Nick Lancaster for providing raw data for particle size distributions of samples across the Namib.

Appendix A. Supplementary data

Supplementary data to this article can be found online at https://doi.org/10.1016/j.qsa.2024.100190.

References

Aitken, M., 1985. Thermoluminescence Dating. Academic Press, London, p. 351.
Andrefsky Jr., W., 2009. The analysis of stone tool procurement, production, and maintenance. J. Archaeol. Res. 17 (1), 65–103. https://doi.org/10.1007/s10814-008-9026-2.
Balescu, S., Lamothe, M., 1994. Comparison of TL and IRSL age estimates of feldspar coarse grains from waterlain sediments. Quat. Sci. Rev. 13, 437–444. https://doi.org/10.1016/0277-3791(94)90056-6.
Besler, H., 1996. The Tsondab Sandstone in Namibia and its significance for the Namib Erg. S. Afr. J. Geol. 99 (1), 77–87. https://hdl.handle.net/10520/EJC-92a7ad2b8.
Besler, H., Marker, M.E., 1979. Namib Sandstone: a distinct lithological unit. S. Afri. J. Geol. 82, 155–160. https://hdl.handle.net/10520/AJA10120750_1045.
BGR, 1998. German-Namibian Groundwater Exploration Project – Technical Cooperation Project No.: 89.2034.0 – Follow up Report Vol.7 – Kuiseb Dune Area/Assessment of the Groundwater Potential (By G. Schmidt).
Bøtter-Jensen, L., McKeever, S.W.S., Wintle, A.G., 2003. Optically Stimulated Luminescence Dosimetry. Elsevier, Amsterdam, p. 375.
Bourke, M.C., Child, A., Stokes, S., 2003. Optical age estimates for hyper-arid fluvial silts at Homeb, Namibia. Quat. Sci. Rev. 22, 1099–1103. https://doi.org/10.1016/S0277-3791(03)00085-4.
Brook, G.A., Cowart, J.B., Brandt, S.A., Scott, L., 1997. Quaternary climatic change in southern and eastern Africa during the last 300 ka: the evidence from caves in Somalia and the Transvaal region of South Africa. Z. Geomophol. Supp 108, 15–48.
Brown, R.W., Rust, D.J., Summerfield, M.A., Gleadow, A.J.W., de Wit, M.C.J., 1990. An early Cretaceous phase of accelerated erosion on the south-western margin of Africa: evidence from apatite fission track analysis and the offshore sedimentary record. Nucl. Tracks Rad. Meas. 17 (3), 339–350. https://doi.org/10.1016/1359-0189(90)90056-4.
Bristow, C.S., Lancaster, N., Duller, G.A.T., 2005. Combining ground penetrating radar studies and optical dating to determine dune migration in Namibia. J. Geol. Soc. London 162, 315–321. https://doi.org/10.1144/0016-764903-120.
Bristow, C.S., Duller, G.A.T., Lancaster, N., 2007. Age and dynamics of linear dunes in the Namib Desert. Geology 35 (6), 555–558. https://doi.org/10.1130/G23369A.1.
Bubenzer, O., Bodeker, O., Besler, H., 2007. A transcontinental comparison between the southern Namib Erg (Namibia) and the southern great Sand Sea (Egypt). Zbl. Geo. Pal. 1, 7–23.
Bullard, J.E., White, K., Livingstone, I., 2011. Morphometric analysis of aeolian bedforms in the Namib Sand Sea using ASTER data. Earth Surf. Process. Landforms 36, 1534–1549. https://doi.org/10.1002/esp.2189.
Burke, K., 1996. The African plate. S. Afr. J. Geol. 99 (4), 341–409.
Burrough, S.L., Thomas, D.S.G., Allin, J.R., Coulson, S.D., Mothulatshipi, S.M., Nash, D. J., Staurset, S., 2022. Lessons from a lakebed: unpicking hydrological change and early human landscape use in the Makgadikgadi basin, Botswana. Quat. Sci. Rev. 291, 107662 https://doi.org/10.1016/j.quascirev.2022.107662.
Carr, A.S., Chase, B.M., Birkinshaw, S.J., Holmes, P.J., Rabumbulu, M., Stewart, B.A., 2023. Paleolakes and socioecological implications of last glacial "greening" of the South African interior. Proc. Natl. Acad. Sci. USA 120 (21), e2221082120. https://doi.org/10.1073/pnas.2221082120.
Carr, A.S., Chase, B.M., Birkinshaw, S.J., Holmes, P.J., Rabumbulu, M., Stewart, B.A., 2024. Paleo-landscapes and hydrology in the South African interior: implications for human history. https://doi.org/10.17159/sajs.2024/17569.
Chandler, C.K., Radebaugh, J., McBridge, J.H., Morris, T.H., Narteau, C., Arnold, K., Lorenz, R.D., Barnes, J.W., Hayes, A., Rodriguez, S., Rittenour, T., 2022. Near-surface structure of a large linear dune and an associated crossing dune of the northern Namib Sand Sea from Ground Penetrating Radar: implications for the history of large linear dunes on Earth and Titan. Aeolian Res 57, 100813. https://doi.org/10.1016/j.aeolia.2022.100813.
Charnay, B., Barth, E., Rafkin, S., Narteau, C., Lebonnois, S., Rodriquez, S., Correch du Pont, S., Lucas, A., 2015. Methane storms as a driver of Titan's dune orientation. Nat. Geosci. 8 (5), 362–366. https://doi.org/10.1038/ngeo2406.
Chase, B.M., Niedermeyer, E.M., Boom, A., Carr, A.S., Chevalier, M., He, F., Meadows, M. E., Ogle, N., Reimer, P.J., 2019. Orbital controls on Namib Desert hydroclimate over the past 50,000 years. Geology 47 (9), 867–871. https://doi.org/10.1130/G46334.1.
Christelis, G., Struckmeier, W., 2001. Groundwater in Namibia, an Explanation to the Hydrogeological Map [HYMNAM/Hydrogeological Map of Namibia 2001], first ed. BGR & DWA & GSN, Windhoek.
Collins, J.A., Schefuß, E., Heslop, D., Mulitza, S., Prange, M., Zabel, M., Tjallingii, R., Dokken, T.M., Huang, E., Mackensen, A., Schulz, M., Tian, J., Zarriess, M., Wefer, G., 2011. Interhemispheric symmetry of the tropical African rain belt over the past 23,000 years. Nat. Geosci. 4, 42–45. https://doi.org/10.1038/ngeo1039.
Collins, J.A., Schefuß, E., Mulitza, S., Prange, M., Werner, M., Tharammal, T., Paul, Wefer, G., 2013. Estimating the hydrogen isotopic composition of past precipitation using leaf-waxes from western Africa. Quat. Sci. Rev. 65, 88–101. https://doi.org/10.1016/j.quascirev.2013.01.007.
Collins, J.A., Schefuß, E., Givon, A., Mulitza, S., Tiedermann, R., 2014. Insolation and glacial–interglacial control on southwestern African hydroclimate over the past 140 000 years. Earth Planet Sci. Lett. 398, 1–10. https://doi.org/10.1016/j.epsl.2014.04.034.
Corvinus, G., 1983. The raised beaches of the west coast of south west Africa. In: Namibia: an Interpretation of Their Archaeological and Palaeontological Data. Munich: CH Beck, p. 112.
Corvinus, G., 1985. An Acheulian industry within the raised Beach complex of the CDM Concession area, SW Africa (Namibia). Quartar 35/36, 183–189. https://doi.org/10.7485/QU35_09.
Coulson, S., Staruset, S., Mothulatshipi, S., Burrough, S.L., Nash, D.J., Thomas, D.S.G., 2022. Thriving in the Thirstland: new stone age sites from the middle Kalahari, Botswana. Quat. Sci. Rev. 297, 107695 https://doi.org/10.1016/j.quascirev.2022.107695.
Daniau, A.-L., Loutre, M.-F., Swingedouw, D., Laepple, T., Bassinot, F., Malaizé, Kageyama, M., Charlier, K., Carfantan, H., 2023. Precession and obliquity forcing of the South African monsoon revealed by sub-tropical fires. Quat. Sci. Rev. 310, 108128 https://doi.org/10.1016/j.quascirev.2023.108128.
Dewar, G., 2008. The Archaeology of the Coastal Desert of Namaqualand, South Africa: a Regional Synthesis, S1761. British Archaeological Reports International Series.
Dewar, G., Stewart, B.A., 2016. Paleoenvironments, Sea Levels, and land Use in Namaqualand, South Africa, during MIS 6-2. In: Jones, S., Stewart, B. (Eds.), Africa from MIS 6-2. Vertebrate Paleobiology and Paleoanthropology. Springer, Dordrecht, pp. 195–212.
Durcan, J.A., King, G.E., Duller, G.A.T., 2015. DRAC: dose rate and age calculator for trapped charge dating. Quat. Geochronol. 28, 54–61. https://doi.org/10.1016/j.quageo.2015.03.012.
Eckardt, F.D., Livingstone, I., Seely, M., Von Holdt, J., 2013a. The surface geology and geomorphology around Gobabeb, Namib Desert. Namibia. Geog. Ann. A 95 (4), 271–284. https://doi.org/10.1111/geoa.12028.
Eckardt, F.D., Soderberg, K., Coop, L.J., Muller, C.C., Vickery, K.J., Grandin, R.D., Jack, C., Kapaklanga, T.S., Henschel, J., 2013b. The nature of moisture at Gobabeb, in the central Namib Desert. J. Arid Environ. 93, 7–19. https://doi.org/10.1016/j.jaridenv.2012.01.011.
Ecker, M., Green, C., Henderson, A., Fual, I., Segadika, P., Mothulatshipip, S., 2023. Archaeological survey near Tsabon6, Kgalagadi District, southwestern Botswana. Azania 58 (4), 517–535. https://doi.org/10.1080/0067270X.2023.2260150.
Garzanti, E., Ando, S., Vezzoli, G., Lustrino, M., Boni, M., Vermeesch, P., 2012. Petrology in the Namib Sand Sea: long-distance transport and compositional variability in the wind-displaced Orange Delta. Earth Sci. Rev. 112, 173–189. https://doi.org/10.1016/j.earscirev.2012.02.008.
Geyh, M.A., Heine, H., 2014. Several distinct wet periods since 420 ka in the Namib Desert inferred from U-series dated of speleothems. Quat. Res. 81, 381–391. https://doi.org/10.1016/j.yqres.2013.10.020.
Gunn, A., 2023. Formation and reorganization time scales of aeolian landscapes. Geology 51 (4), 351–355. https://doi.org/10.1130/G50837.1.
Gunn, A., Casanta, G., Di Liberto, L., Falcini, F., Lancaster, N., Jerolmack, D.J., 2022. What sets aeolian dune height? Nat. Commun. 13, 2401. https://doi.org/10.5281/zenodo.5718792.
Hallinan, E., 2022. "A Survey of Surveys" revisited: current approaches to landscape and surface archaeology in southern Africa. Afr. Archaeol. Rev. 39, 79–111. https://doi.org/10.1007/s10437-021-09469-z.
Hardaker, T., 2011. New approaches to the study of surface Palaeolithic artefacts: a Pilot Project at Zebra river, western Namibia. BAR Int. Ser. 2270.
Hardaker, T., 2020. A Geological explanation for occupation patterns of ESA and early MSA humans in southwestern Namibia? An Interdisciplinary Study. P. Geologist Assoc. 131, 8–18. https://doi.org/10.1016/j.pgeola.2019.10.007.

Hartnady, C.J.H., 1978. The Structural Geology of theNaukluft Nappe Complex, South West Africa Andits Relationship to the Damara Orogenic Belt. Ph.D.thesis. Univ. of Cape Town, Cape Town, South Africa.
Huntley, D.J., Lamothe, M., 2001. Ubiquity of anomalous fading in K-feldspars and the measurement and correction for it in optical dating. Can. J. Earth Sci. 38 (7), 1093–1106. https://doi.org/10.1139/e01-013.
Jouzel, J., Masson-Delmotte, V., Cattani, O., Dreyfys, G., Falourd, S., Hoffman, G., Minster, B., Nouet, J., Barnola, J.M., Chappellaz, J., Fischer, H., Gallet, J.C., Johnsen, S., Leuenberger, M., Loulergue, L., Luethi, D., Oerter, H., Parrenin, F., Raisbeck, G., Raynaud, D., Schilt, A., Schwander, J., Selmo, E., Souchez, R., Spahni, R., Stauffer, B., Steffensen, J.P., Stenni, B., Stocker, T.F., Tison, J.L., Wener, M., Wolff, E.M., 2007. Orbital and millennial antarctic climate variability over the past 800,000 years. Science 317 (5839), 793–796. https://doi.org/10.1126/science.1141038.
Kinahan, J., Kinahan, J.H.A., 2010. The Namib Desert archaeological survey. Antiquity 84, 920–923.
Kinahan, J., 2022. Namib: the Archaeology of an African Desert. University of Namibia Press, Windhoek.
Klein, R.G., 1988. The archaeological significance of animal bones from acheulean sites in southern Africa. Afr. Archaeol. Rev. 6, 3–25. https://doi.org/10.1007/BF01117110.
Kocurek, G., Lancaster, N., Carr, M., Frank, S., 1999. Tertiary Tsondab Sandstone Formation: preliminary bedform reconstruction and comparison to modern Namib Sand Sea dunes. J. Afr. Earth Sci. 29 (4), 629–642. https://doi.org/10.1016/S0899-5362(99)00120-7.
Kolb, T., Fuchs, M., 2018. Luminescence dating of pre-Eemian (pre-MIS 5e) fluvial terraces in Northern Bavaria (Germany) - Benefits and limitations of applying a pIRIR225-approach. Geomorphology 321, 16–32. https://doi.org/10.1016/j.geomorph.2018.08.009.
Korn, H., Martin, H., 1959. Gravity tectonics in the Naukluft Mountains of south west Africa. Geol. Soc. Am. Bull. 70, 1047–1078. https://doi.org/10.1130/0016-7606(1959)70[1047:GTITNM]2.0.CO;2.
Lancaster, N., 1981. Grain size characteristics of Namib Desert linear dunes. Sedimentology 28 (1), 112–115. https://doi.org/10.1111/j.1365-3091.1981.tb01668.x.
Lancaster, N., 1989. The Namib Sand Sea: Dune Forms, Processes and Sediments. Balkema, Rotterdam, p. 180.
Lancaster, J., Lancaster, N., Seely, M.K., 1984. Climate of the central Namib Desert. Madoqua 14 (1), 5–61.
Lancaster, N., Ollier, C.D., 1983. Sources of sand for the Namib Sand Sea. Z Geomorphol. Supp. 45, 71–83.
Laskar, J., Robutel, P., Joutel, F., Gastineau, M., Correia, A.C.M., Levrard, B., 2004. A long term numerical solution for the insolation quantities of the Earth. Astron. Astrophys. 428 (1), 261–285. https://doi.org/10.1051/0004-6361:20041335.
Leader, G.M., Marks, T., Efraim, K., Marais, E., 2022. Anibtanab: an earlier and middle stone age site in the northern Sand Sea. J. Namib. Sci. Soc. 69, 89–102.
Leader, G.M., Bynoe, R., Marks, T., Stone, A., Efraim, K., Stratford, D., Marais, E., 2023. Revisiting the acheulean at Namib IV, Namib Desert, Namibia. J. Field Archaeol. 48 (5), 380–394. https://doi.org/10.1080/00934690.2023.2219102.
Livingstone, I., 2013. Aeolian geomorphology of the Namib Sand Sea. J. Arid Environ. 93, 30–39. https://doi.org/10.1016/j.jaridenv.2012.08.005.
Livingstone, I., Bristow, C., Bryant, R.G., Bullard, J., White, K., Wiggs, G.F.S., Baas, A.C.W., Bateman, M.D., Thomas, D.S.G., 2010. The Namib Sand Sea digital database of aeolian dunes and key forcing variables. Aeolian Res 2, 93–104. https://doi.org/10.1016/j.aeolia.2010.08.001.
Lombard, M., Bradfield, J., Caruana, M.V., Makhubela, T.V., Dusseldorp, G.L., Kramers, J.D., Wurz, S., 2022. The South African Stone Age Sequence updated (II). S Afr. Arch. Bull 77 (217), 172–212.
MacCalman, H.R., Viereck, A., 1967. Peperkorrel, a factory site of Lupemban affinities from central south west Africa. S. Afr. Archaeol. Bull. 22 (86), 41–50. https://doi.org/10.2307/3888081.
Marker, M., 1979. Relict fluvial terraces on the Tsondab flats, Namibia. J. Arid Environ. 2, 113–117. https://doi.org/10.1016/S0140-1963(18)31787-7.
Marks, T.P., 2015. Middle and later stone age land use systems in desert environments: insights from the Namibian surface record. S. Afr. Archaeol. Bull. 70 (202), 180–192. https://www.jstor.org/stable/43869486.
Marks, T., 2018. Bedtime for the Middle Stone Age: Land Use, Stratigraphic Foraging and Lithic Technology at the End of the Pleistocene in the Namib Desert, Namibia. Unpublished. PhD Thesis. Graduate College of The University of Iowa, p. 257.
Marks, T., Marais, E., Seely, M., McCall, G., 2014. Revisiting the early stone age of the Namib Sand Sea: new research at Namib IV and Mniszechi's Vlei. In: Paleoanthropology Society Meeting Abstracts, Calgary, Canada, 8-9th April 2014" PaleoAnthropology 2014:A1-A31.
Mesfin, I., Pluerdeau, D., Forestier, H., 2021. L'assemblage lithique du site Acheuléen de Namib IV (Namib central, Namibie). The lithic assemblage of the Acheulean site of Namib IV (Central Namib, Namibia). L'Anthropologie 125 (1), 102848. https://doi.org/10.1016/j.anthro.2021.102848.
Mesfin, I., Mussgnug, U., Hallinan, E., 2022. Southern African Stone Age archaeology and palaeontology in a mining context: the example of Gudrun Corvinus in the diamond mines of the Sperrgebiet, Namibia (1976–1980). Azania 57 (3), 365–391. https://doi.org/10.1080/0067270X.2022.2115280.
McCall, G.S., Marks, T.P., Thomas, J.T., Eller, M., Horn III, S.W., Horowitz, R.A., Kettler, K., Taylor-Perryman, R., 2011. Erb Tanks: a middle and later stone age rock shelter in the central Namib Desert, western Namibia. PaleoAnthropology 398–421. https://doi:10.4207/PA.2011.ART67.
Miller, R. McG., 2008. The geology of Namibia. Windhoek, Namibia : ministry of mines and energy. Geological Survey 3.
Mitchell, D., Henschel, J.R., Hetem, R.S., Wassenaar, T.D., Strauss, W.M., Hanarahn, S. A., Seely, M.K., 2020. Fog and fauna of the Namib Desert: past and future. Ecosphere 11 (1), e02996. https://doi.org/10.1002/ecs2.2996.
Miyamoto, S., 2010. Late Pleistocene sedimentary environment of the Homeb silts deposits, along the middle Kuiseb River in the Namib Desert, Namibia. Study Monographs Supplementary Issue 40, 19–30.
Muñoz Sabater, J., 2019. ERA5-Land hourly data from 1981 to present. Copernicus Climate Change Service (C3S) Climate Data Store (CDS) 10. https://doi.org/10.14989/96298.
Munyikwa, K., Kinnaird, T.C., Sanderson, D.C.W., 2021. The potential of portable luminescence readers in geomorphological investigations: a review. Earth Surf. Process. Landforms 46, 131–150. https://doi.org/10.1002/esp.4975.
Murray, A., Wintle, A., 2000. Luminescence dating of quartz using an improved single-aliquot regenerative-dose protocol. Radiat. Meas. 32, 57–73. https://doi.org/10.1016/S1350-4487(99)00253-X.
Nash, D.J., Ciborowski, T.J.R., Coulson, S.D., Staurset, S., Burrough, S.L., Mothulatship, S., Thomas, D.S.G., 2022. Mapping Middle Stone Age human mobility in the Makgadikgadi Pans (Botswana) through multi-site geochemical provenancing of silcrete artefacts. Quat. Sci. Rev. 297, 107811 https://doi.org/10.1016/j.quascirev.2022.107811.
Odell, G.H., 2004. Lithic Analysis. Springer Science and Business Media, New York, NY, p. 262.
Picart, C., Dauteuil, O., Pickford, M., Owono, F.M., 2020. Cenozoic deformation of the South African plateau, Namibia: insights from planation surfaces. Geomorphology 35, 106922. https://doi.org/10.1016/j.geomorph.2019.106922.
Prescott, J.R., Hutton, J.T., 1994. Cosmic ray contributions to dose rates for luminescence and ESR dating: large depths and long-term time variations. Radiat. Meas. 23, 497–500. https://doi.org/10.1016/1350-4487(94)90086-8.
Rifkin, R.F., Prinsloo, L.C., Dayet, L., Haaland, M.M., Henshilwood, C.S., Diz, E.L., Moyo, S., Vogelsang, R., Kambombo, F., 2016. Characterising pigments on 30 000-year-old portable art from Apollo 11 cave, Karas region, southern Namibia. J. Archaeol. Sci. 5, 336–347. https://doi.org/10.1016/j.jasrep.2015.11.028.
Roberts, H.M., 2012. Testing Post-IR IRSL protocols for minimising fading in feldspars, using loess with independent chronological control. Radiat. Meas. 47, 716–724. https://doi.org/10.1016/j.radmeas.2012.03.022.
Sanderson, D.C.W., Murphy, S., 2010. Using simple portable OSL measurements and laboratory characterisation to help understand complex and heterogeneous sediment sequences for luminescence dating. Quat. Geochronol. 5, 299–305. https://doi.org/10.1016/j.quageo.2009.02.001.
Schmidt, I., 2011. A middle stone age assemblage with discoid lithic technology from Etemba 14, Erongo Mountains, northern Namibia. J. Afr. Archaeol. 9 (1), 85–100. http://www.jstor.org/stable/43135535.
Seely, M.K., Sandelowsky, B.H., 1974. Dating the regression of a river's end point. S. Afr. Archaeol. Bull. 2, 61–64. https://www.jstor.org/stable/i294365.
Selby, M.J., Hendy, C.H., Seely, M.K., 1979. A late Quaternary lake in the central Namib Desert, southern Africa, and some implications. Palaeogeogr. Palaeoclimatol. Palaeoecol. 26, 37–41.
Senut, B., Pickford, M., 1995. Fossil eggs and Cenozoic continental biostratigraphy of Namibia. Palaeontol. Afr. 32, 33–37.
Shackley, M., 1980. An Acheulean industry with Elephas recki Fauna from Namib IV, south west Africa (Namibia). Nature 284, 340–341.
Shackley, M., 1982. Namib IV and the Acheulean technology complex in the central Namib Desert (south west Africa). Palaeocology of Africa 14 (15), 152–158.
Shackley, M., 1985. Palaeolithic archaeology of the central Namib Desert. Cimbebaisa Memoir 6 (pp84).
Shackley, M., Komura, K., Hayeshi, T., Ikeya, M., Matsu'ura, S., Ueta, N., 1985. Chronometric dating of bone from Namib IV Acheulean site, south west Africa/Namibia. Bull. Natn. Sci. Mus., Tokyo, Ser. D 11, 6–12.
Smedley, R.K., Duller, G.A.T., Pearce, N.J.G., Roberts, H.M., 2012. Determining the K-content of single-grains of feldspar for luminescence dating. Radiat. Meas. 47 (9), 790–796. https://doi.org/10.1016/j.radmeas.2012.01.014.
Southgate, R.I., Masters, P., Seely, M.K., 1996. Precipitation and biomass changes in the Namib Desert dune ecosystem. J. Arid Environ. 33, 267–280. https://doi.org/10.1006/jare.1996.0064.
Staurset, S., Coulson, S.D., Mothulatshipi, S., Burrough, S.L., Nash, D.J., Thomas, D.S.G., 2023a. Making points: the middle stone age lithic industry of the Makgadikgadi basin, Botswana. Quat. Sci. Rev. 30, 107823 https://doi.org/10.1016/j.quascirev.2022.107823.
Staurset, S., Coulson, S.D., Mothulatshipi, S., Burrough, S.L., Nash, D.J., Thomas, D.S.G., 2023b. Post-depositional disturbance and spatial organization at exposed open-air sites: examples from the middle stone age of the Makgadikgadi basin, Botswana. Quat. Sci. Rev. 30, 107824 https://doi.org/10.1016/j.quascirev.2022.107824.
Stone, A., 2013. Age and dynamics of the Namib Sand Sea: a review of chronological evidence and possible landscape development models. J. Afr. Earth Sciences 82, 70–87. https://doi.org/10.1016/j.jafrearsci.2013.02.003.
Stone, A., Thomas, D.S.G., Viles, H.A., 2010. Late Quaternary palaeohydrological changes in the northern Namib Sand Sea: new chronologies using OSL dating of interdigitated aeolian and water-lain interdune deposits. Palaeogeogr. Palaeoclimatol. Palaeoecol. 288, 35–53. https://doi.org/10.1016/j.palaeo.2010.01.032.
Stone, A., Bateman, M.D., Thomas, D.S.G., 2015. Rapid age assessment in the Namib Sand Sea using a portable luminescence reader. Quat. Geochronol. 30, 134–140. https://doi.org/10.1016/j.quageo.2015.02.002.

Stone, A., Bateman, M.D., Burrough, S.L., Garzanti, E., Limonta, M., Radeff, G., Telfer, M. W., 2019. Using a portable luminescence reader for rapid age assessment of aeolian sediments for reconstructing dunefield landscape evolution in southern Africa. Quat. Geochronol. 49, 57–64. https://doi.org/10.1016/j.quageo.2018.03.002.

Stone, A., Nitundul, S., Bateman, M., Sanderson, D., Cresswell, Srivastava, A., Kinnaird, T., 2023. Exploring dryland dynamics with portable luminescence readers: the good, the bad and the ugly. In: 17th International Conference on Luminescence and Electron Spin Resonance Dating, 25-30th July, 2023, Copenhagen, Denmark.

Stone, A., Bateman, M.D., Sanderson, D., Burrough, S.L., Cutts, R., 2024. Probing sediment burial age, provenance and geomorphic processes in dryland dunes and lake shorelines using portable luminescence data. Quat. Geochronol. QUAGEO-D-23-00093R1.

Stuut, J.-B., Prins, M.A., Schneider, R.R., Weltje, G.J., Jansen, J.H.F., Postma, G., 2002. A 300-kyr record of aridity and wind strength in southwestern Africa: inferences from grain-size distributions of sediments on Walvis Ridge, SE Atlantic. Marine Geol. 180, 221–233. https://doi.org/10.1016/S0025-3227(01)00215-8.

Tadono, T., Ishida, H., Oda, F., Naito, S., Minakawa, K., Iwamoto, H., 2014. Precise global DEM generation by ALOS PRISM. Int. Soc. Photogramme. 2 (4), 71–76. https://doi.org/10.5194/isprsannals-II-4-71-2014. https://ui.adsabs.harvard.edu/link_gateway/2014ISPAn.II4...71T/.

Teller, J.T., Lancaster, N., 1986. Lacustrine sediments at Narabeb in the central Namib Desert, Namibia. Palaeogeogr. Palaeoclimatol. Palaeoecol. 56, 177–195. https://doi.org/10.1016/0031-0182(86)90093-3.

Teller, J.T., Lancaster, N., 1987. Description of late Cenozoic lacustrine sediments at Narabeb, central Namib Desert. Modoqua 15, 163–167.

Teller, J.T., Rutter, N., Lancaster, N., 1990. Sedimentology and paleohydrology of late Quaternary lake deposits in the northern Namib Sand Sea, Namibia. Quat. Sci. Rev. 9, 343–364. https://doi.org/10.1016/0277-3791(90)90027-8.

Thomas, D.S.G., Burrough, S.L., Coulson, S.D., Mothulatshipi, S., Nash, D.J., Staurset, S., 2022. Lacustrine geoarchaeology in the central Kalahari: implications for Middle Stone Age behaviour and adaptation in dryland conditions. Quat. Sci. Rev. 297, 107826 https://doi.org/10.1016/j.quascirev.2022.107826.

Thomas, D.S.G., Bynoe, R., 2023. Life on the edge or living in the middle? New perspectives on southern Africa's Middle Stone Age. Quat. Sci. Rev. 303, 107965. https://doi.org/10.1016/j.quascirev.2023.107965.

Thomsen, K.J., Murray, A.S., Jain, M., Bøtter-Jensen, L., 2008. Laboratory fading rates of various luminescence signals from feldspar-rich sediment extracts. Radiat. Meas. 43 (9–10), 1474–1486. https://doi.org/10.1016/j.radmeas.2008.06.002.

Todd, N.E., 2005. Reanalysis of African Elephas recki: implications for time, space and taxonomy. Quat. Int. 126, 65–72. https://doi.org/10.1016/j.quaint.2004.04.015.

Trauerstein, M., Lowick, S.E., Preusser, F., Rufer, D., Schlunegger, F., 2012. Exploring fading in single grain feldspar IRSL measurements. Quat. Geochronol. 10, 327–333. https://doi.org/10.1016/j.quageo.2012.02.004.

Van der Wateren, F.M., Dunai, T.J., 2001. Late Neogene passive margin denudation history -cosmogenic isotope measurements from the central Namib desert. Global Planet. Change 30, 271–307. https://doi.org/10.1016/S0921-8181(01)00104-7.

Vermeesch, P., Fenton, C.R., Kober, F., Wiggs, G.F.S., Bristow, C.S., Xu, S., 2010. Sand residence times of one million years in the Namib Sand Sea from cosmogenic nuclides. Nat. Geosci. 3, 862–865. https://doi.org/10.1038/ngeo985.

Viola, G., Mancktelow, N.S., Miller, J.A., 2006. Cyclic frictional-viscous slip oscillations along the base of an advancing nappe complex: insights into brittle-ductile nappe emplacement mechanisms from the Naukluft Nappe Complex, central Namibia. Tectonics 25 (3), TC3016. https://doi.org/10.1029/2005TC001939.

Vogelsang, R., 1998. Middle-Stone-Age-Fundstellen in Südwest-Namibia. Heinrich-Barth Institute, Cologne.

Vogelsang, R., Richter, J., Jacobs, Z., Eichhorn, B., Linseele, V., Roberts, R.G., 2010. New excavations of middle stone age deposits at Apollo 11 rockshelter, Namibia: stratigraphy, archaeology, chronology and past environments. J. Afr. Archaeol. 8 (2), 185–218. https://www.jstor.org/stable/43135517.

Ward, J.D., 1984. Aspects of the Cenozoic Geology in the Kuiseb Valley, Central Namib Desert. PhD. thesis (unpublished) University of Natal, Pietermaritzburg. p.310.

Ward, J.D., 1987. The Cenozoic succession in the Kuiseb valley, central Namib Desert. Geological Survey of South West Africa Memoir 9 (pp124).

Ward, J.D., 1988. Eolian, fluvial and pan (playa) facies of the Tertiary Tsondab Sandstone Formation of the central Namib Desert, Namibia. Sediment. Geol. 55, 143–162. https://doi.org/10.1016/0037-0738(88)90094-2.

Ward, J.D., Corbett, I., 1990. Towards an age for the Namib. In: Ward, J.D., Corbett, I., Seely, M.K. (Eds.), Namib Ecology: 25 Years of Namib Research. Transvaal Museum, Pretoria, pp. 17–26.

Ward, J.D., Seeley, M.K., Lancaster, N., 1983. On the antiquity of the Namib Desert. South Afr. J. Sci. 79, 175–183.

Wasson, R.J., Hyde, R., 1983. Factors determining desert dune type. Nature 304, 337–339. https://doi.org/10.1038/304337a0.

Wendt, W.E., 1972. Preliminary report on an archaeological research programme in South West Africa. CIMBEBASIA 2, 1–61.

Wendt, W.E., 1976. Art mobilier from the Apollo 11 Cave, Southwest Africa: Africa's oldest dated works of art. S. Afr. Archaeol. Bull. 31, 5–11. https://doi.org/10.2307/3888265.

Wintle, A.G., Murray, A.S., 2006. A review of quartz optically stimulated luminescence characteristics and their relevance in single-aliquot regeneration dating protocols. Radiat. Meas. 41 (4), 369–391. https://doi.org/10.1016/j.radmeas.2005.11.001.

Wroth, K., Tribolo, C., Bousmna, C.B., Horwitz, L.K., Rossouw, L., Miller, C.E., Toffolo, M.B., 2022. Human occupation of the semi-arid grasslands of South Africa during MIS 4: new archaeological and paleoecological evidence from Lovedale, Free State. Quat. Sci. Rev. 283, 107455 https://doi.org/10.1016/j.quascirev.2022.107455.

Yamagata, K., Mizuno, K., 2005. Landform development along the middle course of the Kuiseb River in the Namib Desert, Namibia. Afr. study Monogr. Suppl. issue 30, 15–25. https://doi.org/10.14989/68464.